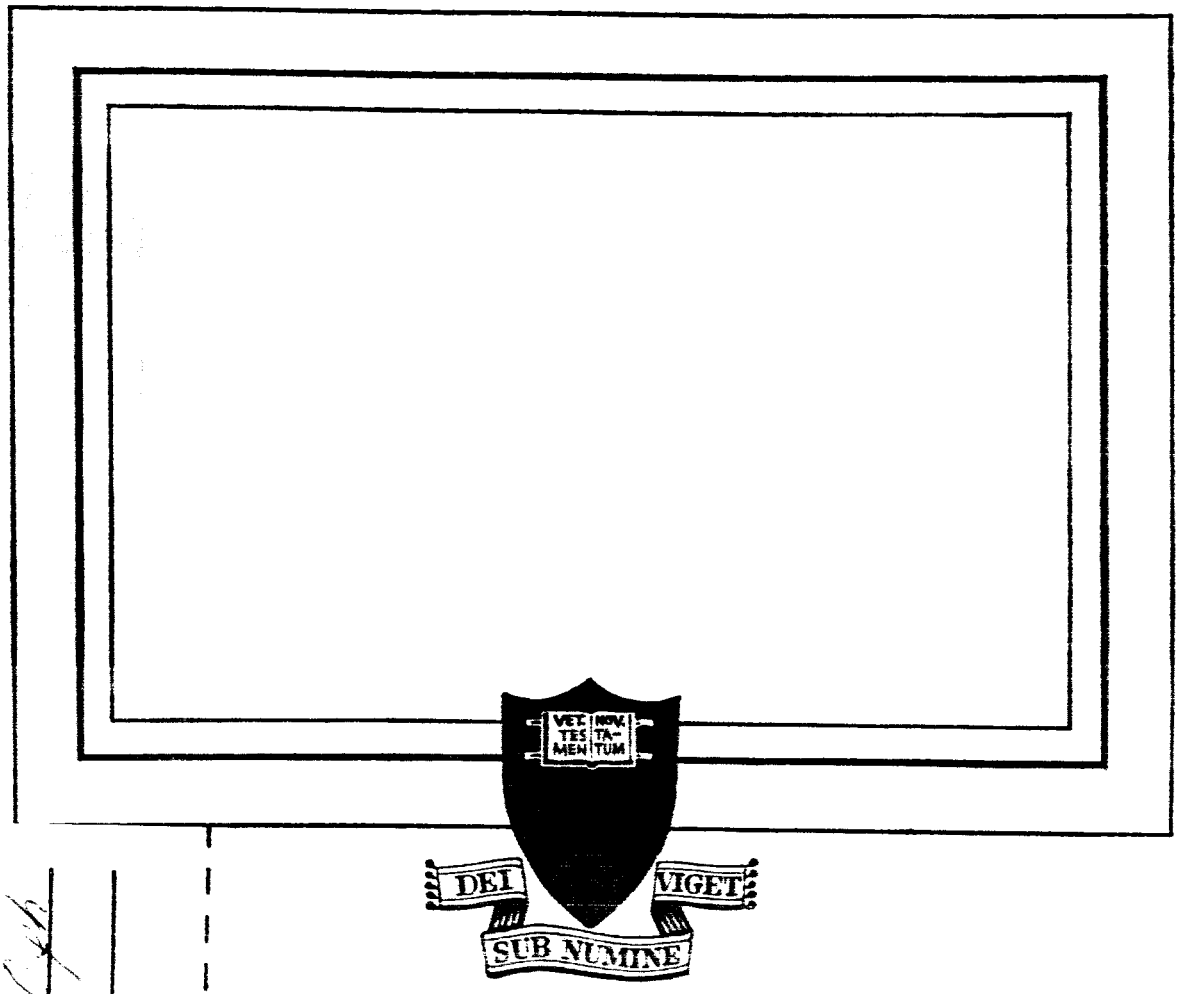

PRINCETON UNIVERSITY

DEPARTMENT OF AEROSPACE AND MECHANICAL SCIENCES

NATIONAL AERONAUTICS
AND SPACE ADMINISTRATION

Research Grant NsG-306-63

PULSED ELECTROMAGNETIC GAS ACCELERATION

Fourth Semi-Annual Progress Report

1 January 1964 to 30 June 1964

Report No. 634c

Prepared by: Robert G. Jahn
Robert G. Jahn
Associate Professor
and Research Leader

and: Woldemar v. Jaskowsky
Woldemar F. von Jaskowsky
Research Engineer

with contributions from the staff.

31 July 1964

Guggenheim Laboratories for the Aerospace Propulsion Sciences
Department of Aerospace and Mechanical Sciences
PRINCETON UNIVERSITY
Princeton, New Jersey

ABSTRACT

29689

Experimental study of the initiation and development of the current pulses in large-radius pinch discharges has been facilitated by the construction of a 5-inch, tubular, pinch-generating device. This machine is capable of producing essentially impermeable, cylindrical current sheets which are coupled to the external circuit over most of their inward excursion. Streak and Kerr-cell photography, photoelectric spectroscopy, magnetic and electric probes have revealed many of the interior details of these current pulses and an auxiliary electrode containing a central orifice leading to a glass vacuum chamber has permitted optical observation of the exhaust plume.

A lumped-line type of pulse-forming circuit has been developed to drive another discharge chamber. This device permits the application of current and voltage waveforms of prescribed profiles to the pinch discharges. Microwave probing of the precursor regions of the 8-inch discharges continues, as does the development of double Langmuirprobes, small Rogowski probes, and power-balance determinations. Analytical study of cylindrical shock processes and three-fluid hydromagnetic models to supplement earlier snow-plow concepts is in progress.

Author

TABLE OF CONTENTS

		Page
	TITLE PAGE	i
	ABSTRACT	ii
	TABLE OF CONTENTS	iii
	LIST OF ILLUSTRATIONS	iv
I.	INTRODUCTION	1
II.	THE TUBULAR PINCH MACHINE	1
	A. Description	1
	B. External Circuit Characteristics	2
	C. Streak Photographs	3
	D. Kerr-Cell Photographs	3
	E. Spectroscopy	4
	F. Current Density Distributions	6
III.	MICROWAVE STUDIES	7
IV.	DISCHARGES WITH EXHAUST	9
V.	PULSE FORMING MACHINE	9
VI.	PROGRESS ON RELATED STUDIES	11
VII.	SUMMARY AND PROJECTION	13
	REFERENCES	14
	APPENDIX I	
	Pulse-forming Network Calculations	16
	APPENDIX II	
	Semi-Annual Statement of Expenditures	17
	ILLUSTRATIONS, Figures 1 to 25	

LIST OF ILLUSTRATIONS

FIGURE

1 Tubular Plasma Pinch Apparatus (Schematic)

2 View of Tubular Plasma Pinch Apparatus

3 Streak Photographs of Pinch Discharge in Argon --- 5" Tubular Machine

4 Streak Photographs of Pinch Discharge in Argon --- 8" Machine

5 Axial Photographs of 5" Pinch Discharge 1920 μ Argon; 0.05 μ sec. Exposure

6 Perspective Photographs of 5" Pinch Discharge 1920 μ Argon; 0.05 μ sec. Exposure

7 Axial Photographs of 5" Pinch Discharge 480 μ Argon; 0.05 μ sec. Exposure

8 Perspective Photographs of 5" Pinch Discharge 480 μ Argon; 0.05 μ sec. Exposure

9 Axial Photographs of 5" Pinch Discharge 120 μ Argon; 0.05 μ sec. Exposure

10 Perspective Photographs of 5" Pinch Discharge 120 μ Argon; 0.05 μ sec. Exposure

11 Axial Photographs of 5" Pinch Discharge 30 μ Argon; 0.05 μ sec. Exposure

12 Perspective Photographs of 5" Pinch Discharge 30 μ Argon; 0.05 μ sec. Exposure

13 5" Discharge in 120 μ Argon at $R/R_o = \frac{1}{2}$

14 5" Discharge at $R/R_o = \frac{1}{2}$

15 Current Density Distributions in 5" Pinch Discharge in 120 μ Argon

16 8" Plasma Pinch Chamber with Electrode for Micro Wave Probing

17 Upper: Response of 70 Gc Micro Wave Probe in 8" Pinch Discharge
Lower: Current in Same

LIST OF ILLUSTRATIONS-contd.

FIGURE

18 8" Pinch Discharge in Argon: Time to ½ Max. Reflection of 70 Gc

19 8" Pinch Discharge in Argon: Ionization Time vs. Radial Position, 70 Gc

20 View of Tubular Pinch Discharge Apparatus With Exit Orifice and Exhaust Chamber

21 Photograph of Exhaust from 5" Pinch Discharge in 120 μ Argon

22 Streak Photograph of Exhaust from 5" Pinch Discharge in 120 μ Argon

23 Pulse Forming Plasma Pinch Apparatus (Schematic)

24 Equi-Section Lines

25 Typical Five-Section Current Wave Forms

I. INTRODUCTION

The purpose of this program, and its accomplishments prior to the current reporting period are discussed in detail in several status reports, technical society reprints, and journal publications, all previously submitted to the project file. (1-15); these will not be reviewed here. Suffice it to say that the start of this reporting period found the project with a variety of plasma pinch-generating apparatus and associated diagnostic equipment which had already permitted extensive experimental study of the details of the initiation, stabilization, and acceleration of large-radius pinch discharges. The understanding provided by these experiments and by related theoretical studies had fostered the design and construction of new discharge devices which would more efficiently accelerate the ambient gases, and of new diagnostic tools which would better probe them. This status report is largely devoted to the recent progress with these new devices.

II. THE TUBULAR PINCH MACHINE

A. Description

The first major changes in the design of the pinch-generating apparatus used since the start of this program were incorporated into a 5" diameter, concentric-lead discharge device shown in Figs. 1 and 2. The essential differences between this machine and its predecessors are 1) the use of a lower inductance, coaxial external lead configuration, and lower inductance capacitor terminals to improve the electrical match between the circuit and the discharge; 2) the use of a gas triggered, direct-pinch switch mounted tandem to the main discharge chamber to lower the circuit inductance further and to permit identical discharge initiation patterns in the switch and main chamber; and 3) the reduction of the chamber diameter from 8" to 5" to increase the electrical energy density in the discharge sheets (i.e. increase the $|\beta| = \frac{Q_o^2}{4\pi^2 \rho_o r_o^4}$ parameter, Ref. 11) and allow the first sheet to penetrate further to the center of the chamber before external current reversal. The extent to which these purposes were achieved is indicated by the following summary of the early data obtained from this machine.

B. External Circuit Characteristics

Table I summarizes the comparative performances of the tubular machine and the original 8" diameter plate-lead devices.

Table I

	8" Plate Lead	5" Tubular
Capacitance	15.7 μfd	15.7 μfd
Bank Voltage	10,000 v	10,000 v
Total Inductance	35 nh	9.5 nh
Chamber Inductance	3 nh	3.5 nh
Ringing Frequency	200 KC/sec	410 KC/sec
Total Real Impedance	7×10^{-3} ohm	1.2×10^{-2} ohm
Chamber Real Impedance	3×10^{-3} ohm	5×10^{-3} ohm
Peak Current	2×10^{5} amp	3×10^{5} amp
Peak Current Rise	4×10^{11} amp/sec	1×10^{12} amp/sec
Peak Chamber Voltage	900 v	3,000 v
Time-to-pinch:		
argon, 30 μ	4.2 μsec	1.1 μsec
120 μ	7.2	1.4
480 μ	15.8	3.0
1920 μ	30.5	5.5

It will be noted that the ratio of chamber inductance to total circuit inductance has been increased from less than 10% to more than 35%, permitting a correspondingly large fraction of the capacitor bank energy to be delivered to the main discharge. That this is indeed occurring is indicated by the equivalent increase in the fraction of bank voltage which appears across the chamber electrodes. The lower total circuit inductance is seen to manifest itself in a higher ringing frequency, higher peak current, and perhaps most important, in a higher current rise rate. Comparison of the times-to-pinch for the two machines, when normalized to a common radius, give a quick indication of how much more

effectively the self-generated field is accelerating the discharge sheet. More significant indications will be discussed later in terms of the detailed shapes of the current density pulses, and the comparison of the trajectories of these pulses with the appropriate snow-plow calculations to yield effective sweeping efficiencies.

C. Streak Photographs

As was the case with the earlier machines, study of the development of the luminous phenomena within the discharge is most readily accomplished by direct high-speed photography, either via a rotating mirror camera, or with a Kerr-cell electrical shutter. Typical streak photographs taken through a diametral slot in the positive (ground) electrode of the new machine are shown in Fig. 3, for various ambient argon pressures of interest. Comparison of these with similar streak photographs taken in the earlier machines (Fig. 4) reveal that the luminous fronts are propagating significantly faster in the new device, that they are accelerating over larger fractions of their radial excursions, and that the secondary discharges, if they occur at all, are far less pronounced. Despite their higher velocities, the effective luminosity of these fronts is noticeably greater at all but the lowest pressure ($\sim 30\mu$) where the front is found to be somewhat diffuse. Comparison of these luminous front trajectories with those of the current pulses will be discussed below.

D. Kerr-Cell Photographs

Again drawing on the experience with the larger discharge chambers, a special outer electrode containing a 3" diameter glass insert was constructed for the tubular machine, and through it a sequence of full-field Kerr-cell photographs obtained (Figs. 5-12). As before, these display the remarkable cylindrical symmetry of the luminous fronts, and their insensitivity to small perturbations which may arise at random angular locations on their perimeter. They also display the dependence of the luminous structure on ambient pressure. At the higher pressures, 480μ and 1920μ, the leading edge of the front is sharply defined, and the intensity decays behind it, much like shock tube profiles of luminosity behind very strong shock waves in argon. At 120μ, the leading edge is more diffuse, as might be anticipated from the longer mean free paths prevailing at this pressure. At still lower initial pressure, 30μ, the entire nature of the discharge seems to have changed. Although a gross cylindrical symmetry is still evident, the luminosity now has a wispy, diffuse structure showing little definition of

a propagating leading edge. With this exception, the observed positions of the luminous fronts on these Kerr-cell photographs correlate well with the streak trajectories.

E. Spectroscopy

The photographic observation of the luminous fronts described above reveals much about the geometry, dynamics, and stability of the pinch phenomena under study. More detailed, spectroscopic study of these same fronts should yield additional information about the particle densities, temperatures, and kinetic processes of the various species participating therein. Time-integrated spectra of argon, nitrogen, and helium discharges in the 8" machines had been obtained previously (4, 5), and indicated the presence of neutral, singly and doubly ionized atomic lines, and free-free electron continuum in the discharge radiation. To a certain extent it was possible to localize the main source of each type of radiation, e.g. to the pinch column at the center, to the outer edge, etc., but no finer spatial resolution had been attempted.

Recently, however, an experiment has been undertaken to follow in detail the progression of various spectral lines and continuum through the luminous fronts, by photoelectric monitoring of the appropriate spectral region at various radial positions in the tubular discharge chamber. For example, in one series of discharges in 120 μ argon, the intensities of one each of the emitted AI, AII, and AIII lines, and a representative portion of the continuum radiation was observed simultaneously with the total light profile at the half radius position by type 1P28 photomultipliers, whose output was displayed as a function of time on a dual beam oscilloscope. The total light signal, which functioned both as an intensity normalization and as a local time calibration for each of the other signals, was obtained by reflecting a small fraction of the light out of the optical beam with a thin glass plate. The remaining bulk of the light flux continued through a grating monochomator to another photomultiplier observing the calibrated exit slit.

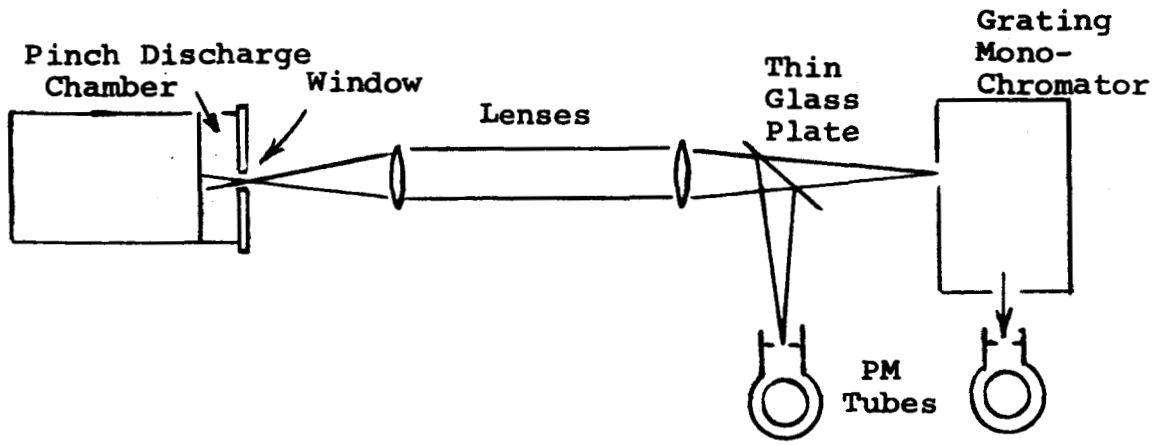

For this particular study, the following lines were found most suitable; AI: 4522.32Å; AII: 4,764.89Å; AIII: 3336.13Å. For the continuum, the region around 4750Å was found to be well free of other lines. The presence of a line, or the absence of nearby lines for the continuum measurement, was established by recording the emitted intensity in overlapping wavelength bands at 2 to 4 Å intervals at 5 settings near the location of the line.

Figure 13 shows the intensity of the radiation of the AII, AIII, and of the continuum, relative to the total light, as the luminous front passes the one-half radius location. The AII intensity is seen to reach a peak measurably ahead of that of the total light signal and before any continuum radiation is observed. The continuum intensity rises and peaks simultaneously with the AIII and with the total light approximately 0.15 μsec after the AII peak. As confirmation of this displacement, the small contribution of the continuum at the AII line wavelength, can be seen superimposed on the back of the AII line profile.

The early part of the luminous front thus appears to be composed primarily of AII radiation, while the subsequent, major portion consists of continuum and AIII radiation. (AI radiation could not be detected within the luminous front.) For the intensity scale used in Fig. 13, the ratio of AII to AIII intensity is ≈ 7 at the time of peak AII intensity; it is $\approx \frac{1}{2}$ in the center of the total luminous front.

Unique interpretation of these profiles is not possible without other complementary information, but certain self-consistent models can be proposed. For example, the initial rise of AII may indicate an increase in the level of first ionization caused by a corresponding rise in electron or gas temperature, or may be indicative of an isothermal relaxation profile, or may simply reflect a compression of the radiating species. The subsequent simultaneous decay of AII and rise of AIII and continuum intensities seems to indicate a process of second ionization of AII into AIII, again caused either by a continuation of the electron or gas temperature increase, or by a second ionization relaxation process. The low level of intensities in the wake of the main pulse may be indicative of a low particle density, or of a low temperature in this region, with the former more likely, since the continuum radiation, which is relatively insensitive to temperature, is also very low here.

The separation of the peak of the AII intensity ahead of the AIII and continuum peaks is not observed at this position for other pressures of discharge (cf. Fig. 14).

At 30μ of argon, for example, the AII intensity stays nearly constant through the total luminous front, an observation which seems inconsistent with the growth of total light through the same region. It may be that the loss of AII density due to second ionization is fortuitously just compensated by a compression of the species in the luminous front.

An additional point of interest in the 30μ profiles is the presence of strong AII radiation, and therefore of ionization, at this half-radius position, at a time after breakdown of only 0.06 μsec -- long before the arrival of the main luminous front. This may be related to the ionization precursor phenomena first discovered with the microwave probe (4, 5), and discussed further in section 7.

Clearly, many further studies of this sort will be needed to complete the picture of ionization kinetics in the luminous fronts. Unfortunately, this particular experiment operates in a marginal signal/noise domain, and considerable patience is required to produce unambiguous data. As more is accumulated, further interpretation will be attempted.

F. Current Density Distributions

The ultimate criterion for the suitability of a particular discharge device to the broad purpose of this program lies in the detailed structure of the current pulses it generates. In particular, it is desired to produce pulses which originate close to the outer wall of the chamber, accelerate to the proper radial speeds, efficiently sweep the ambient gas ahead of them, and remain coupled to the external circuit over their entire inward excursion. The current sheets in the earlier devices accomplished these goals only partially. Notable among their deficiencies were the occurrence of secondary "crow-bar" breakdowns at the outer wall at the time of current reversal in the external circuit, which occurred before the first sheet had propagated more than a fraction of the way to the center at all pressures, and a degree of porosity in the sweeping action of the current pulse piston on the ambient gas. These have been discussed extensively in recent publications (12, 13).

The new tubular 5" machine has been found to produce substantially superior current pulses by all of the above standards. Fig. (15) displays a sequence of current density profiles obtained by the usual magnetic probe mapping techniques (4), for discharges in 120μ argon. It will be noted that the current pulse arises quite near the outer wall, rapidly intensifies to a well-defined intense profile which sweeps

inward at about 5×10^4 m/sec, nearly reaching the center before any significant current reversal occurs in the external circuit.

The sweeping efficiency of this pulse, inferred by comparison of its trajectory with those predicted by modified snow-plow theory (12, 13), is essentially 100%, within experimental error. Perfect sweeping is likewise found in 30μ and 480μ discharges in the same device. Only at ambient pressures as high as 2 mm does a noticeable degree of porosity appear in this machine.

A complete presentation of all current density profile results from this device, along with comparisons of their trajectories with the snow-plow calculations, and with those of the luminous fronts, will be the subject of a separate paper to be presented and published shortly.

III. MICROWAVE STUDIES

Many of the early streak photographs, and certain of the Kerr-cell photographs of the interaction of the discharges with obstacles placed in the chamber, indicated the existence of some type of precursor signal or front, propagating ahead of the main luminous front, and many times faster than it (6). This precursor deserves further study, since, in its privileged position as the first apparent dynamic effect associated with the pinch, it may exert an appreciable influence over phenomena which develop later in the discharge. For example, preliminary experiments with rudimentary microwave probes revealed free-electron densities in this precursor region in the range of $10^{13} cm^{-3}$, corresponding to an ionization of the ambient gas of a few percent. The existence of this low level of ionization ahead of the main current sheet will considerably accelerate the ionization rate in the sheet over that which would prevail if it propagated into a completely unionized gas, since the highly efficient electron-atom collisions can immediately begin the ionization cascade.

A well-designed millimeter microwave probe is a reasonable tool for study of this precursor region, first because the primary manifestation of the front is via the appearance of significant free-electron densities, and second because this device exerts a minimum of disturbance on the region of gas under study. A wavelength of 4 mm. was selected as a compromise among adequate spatial resolution, a satisfactory match to the electron densities prevailing in the region of interest, and the availability of sufficiently reliable signal sources.

A special horn antenna was designed and fabricated by Technical Research Group of Boston. This horn was matched to

free space with a reflected voltage standing wave ratio of better than 1.01 by a quartz element cemented to its mouth. A special upper electrode was constructed for the 8" machine to accept this horn at various radial positions (Fig. 16).

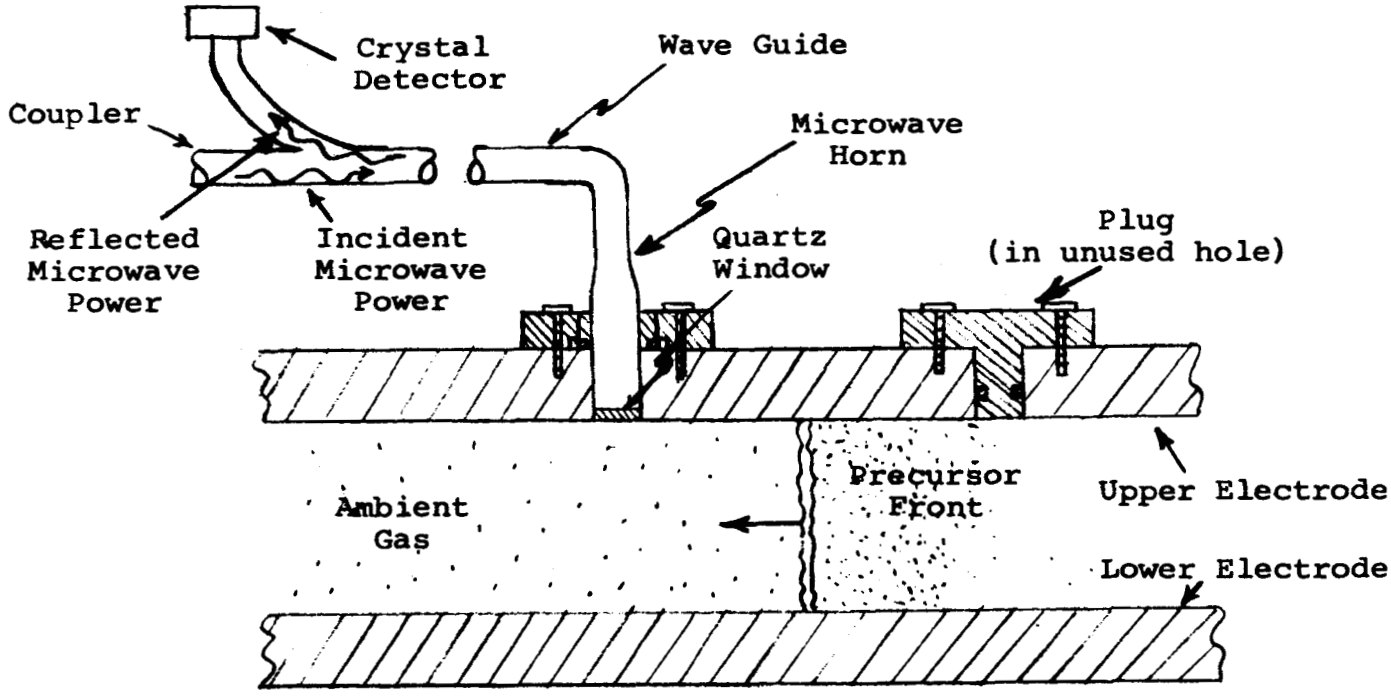

In operation, the microwave power reflected from the ionized gas passing the horn aperture is monitored by a 10 DB directional coupler whose output is displayed on a dual beam oscilloscope simultaneously with some time calibration signal, such as the main Rogowski coil. A typical response of this system to the passage of the precursor front is shown in Fig. 17. From a succession of such records obtained at various radial positions, it is possible to plot trajectories of the precursor front, and to determine its velocity of propagation. Figure 18 displays such trajectories for discharges in four different pressures of argon.

Note that only at the higher pressures is a finite propagation speed well defined, in this case greater than .01 x the speed of light. At the lower pressures, the precursor signal arises simultaneously over the whole chamber, within experimental error, at some well-defined interval after breakdown initiation.

On a much longer time scale, the microwave probe has also permitted study of the duration of ionization in the chamber after completion of the manifest dynamical events in the discharge. Ionization duration times are found to be

dependent on gas type and initial pressure, but are typically of the order of milliseconds for ionization to decay to 1%. By contrast, all of the energy has been put into the gas, in the current sheets, in about 1% of this time, i.e. $\sim$10 μsec. Figure 19 displays certain results of this type of study.

The early results outlined above have encouraged a more detailed series of microwave probe experiments. An extensive survey to map the structure of the precursor region is currently under way. Results will be reported in a separate publication.

IV. DISCHARGES WITH EXHAUST

Our most recent proposal (10) discusses in detail the need to study the effect of an exhaust orifice on the development of the discharges in the pinch configuration, and outlines a series of experiments leading ultimately to the design and construction of a thrust producing configuration. It has been possible to begin this phase of the program somewhat ahead of the proposed schedule, and preliminary results are now being accumulated. Figure 20 is a photograph of the first device employed in this study. The tubular 5" machine has been equipped with an outer electrode which can accept a variety of orifice and nozzle shapes as interchangeable plugs on the centerline. An exhaust chamber is formed by a 2' or 4' length of 6" diameter pyrex pipe extending axially outward from the outer electrode face, which permits photographic observation of the development of the exhaust plume. To date, only a simple 3/4" diameter straight orifice has been used as the exhaust port, and only a few Kerr-cell and streak photographs attempted. Figure 21 shows a time-integrated photograph of the discharge in 120μ argon. Figure 22 is a streak photograph of the same type of discharge, taken along the axis from the orifice out into the exhaust chamber. Such photographs have also been obtained in 30μ, 480μ and 1920μ discharges, and in each case, the initial exhaust velocity is found to be a significant fraction of the sweeping velocity prevailing inside the chamber prior to the pinch. Extension of these studies, including detailed probing of the exhaust plume, and interior of the discharge near the orifice will be a major activity for the coming period.

V. PULSE FORMING MACHINE

The recent proposal (10) also discusses in detail the need for a device which, rather than subjecting the discharge to the free-ringing pattern of a simple L-C-R circuit, would

permit "tailored" pulses of prescribed waveforms to be applied. In this way the dynamical interactions between the current pulses and their driving fields could be optimized over the entire inward excursion. This aspect of the program is also somewhat ahead of the proposed schedule, but unlike the orifice study, its first phase, of necessity, has been primarily analytical. Only recently has the experimental design been established and a device constructed, and this has yet to be fired.

The analytical development of technique for accomplishing the desired pulse programming is an interesting problem in its own right and seems not to have been treated in the literature for the domains of interest. The essential complications arise from the severe demands on current rise times and peak currents needed in the desired output pulses. Specifically, we would like currents rising in a small fraction of a microsecond to levels of 10^5 amps or greater, and remaining tolerably flat-topped for a few microseconds.

In order to retain a maximum degree of flexibility of manipulation in the experimental device, it was decided to restrict consideration to L-C ladder types of lumped transmission lines, composed of identical inductance and capacitance units, which could, however, be assembled in a variety of permutations of the components. Samples of the calculations required to design such a circuit are included in the Appendix; a detailed presentation will be made in a forthcoming Ph.D. thesis.

Figure 23 is a drawing of the pulse-forming device designed on this basis and now being assembled. The chamber and switch are 8" in diameter, but otherwise identical to the 5" tubular machine. The transmission lines take the form of two sets of parallel plates extending about 10' radially outward at 180^0. 20 Aerovox capacitors can be arranged with a variety of spacings along the edges of these plates to provide the desired wave shapes. These capacitors are rated at 2.5 μfd, with self inductances of about 10 nh. If assembled as two parallel 10-element equi-section lines, each will have a nominal impedance of 0.12 ohm, and provide a 6 microsecond pulse of about 10^5 amps.

The response of the discharge to this type of pulse is difficult to anticipate. To the extent that the development of the discharge itself participates in the circuit characteristics, some "iteration" of the passive circuit elements may be necessary to achieve the desired pulse shape.

VI PROGRESS ON RELATED STUDIES

In addition to the major efforts discussed above, several individual experiments and theoretical studies have recently been undertaken in the hope that new tools and techniques will emerge to illuminate further the broad phenomena understudy. It is premature to display results or conclusions from any of these, but the topics are listed here for completeness:

A) Rogowski Probe: A variety of very small Rogowski coils, ranging in size from a few millimeters to more than a centimeter in diameter have been wound on suitable frames and enclosed in glass or epoxy insulation. When inserted into the discharge, these probes respond to the time derivative of the total current passing through their toroidal aperture. As such they provide a useful supplement the data returned by the simple magnetic probes. Their advantage lies in their ability to respond directly to current densities, rather than requiring a tedious cross-plotting and differentiation of magnetic field data as do the simple magnetic probes. Their disadvantage is in the difficulty of constructing them on a sufficiently fine scale that they provide adequate spatial resolution without seriously distorting the region which they probe. At present the emphasis is on the development of satisfactory fabrication techniques.

B) Electric Probes: A variety of double Langmuir probes have been constructed and inserted into the chamber in the hope of obtaining independent information on the development of the ionization patterns within the discharge. Both coaxial and parallel-needle configurations have been tried, and the latter have proved more satisfactory from a gasdynamic standpoint. Considerable early difficulty with rf noise isolation has been overcome with suitably balanced and shielded transformer-coupled circuits, and reproducible data is currently being accumulated and studied. The detailed results will be presented shortly in a master's thesis and separate technical report.

C) Power Inventory: Simultaneous dual beam oscilloscope records of the voltage and current profiles developed across the discharge can be multiplied manually to yield information on the total power input to the gas as a function of time. This may then be compared with energy remaining in the capacitors at the same times to provide a history of the energy utilization. First attempts of this type emphasized the importance of an extremely accurate time correlation between the two oscilloscope traces, particularly in the establishment of a commontime zero. This requirement appears to exceed the inherent linearity and

reproducibility of the oscilloscope sweep circuitry, and hence an auxiliary time mark generator has been constructed to blank both oscilloscope beams at common, one microsecond intervals. With this improvement, new data is now being obtained and reduced.

D) Cylindrical Shock Theory: As a first step toward improvement of the rudimentary snow-plow theory that has been the basis for previous experimental comparison, a sequence of cylindrical shock wave models is being studied. In one, a radial trajectory is assumed for an impermeable piston, and the corresponding shock wave strength and trajectory, and the self-consistent gas flow profile evaluated. In another, a given pulse of energy is applied uniformly at the outer radius, and the subsequent implosion wave structure is evaluated. Ultimately it is hoped to combine the two extremes to provide parametric models closely resembling the gasdynamic aspects of the pinch discharges.

E) Three-Fluid Theory: A more ambitious theoretical formulation has been undertaken, based on simultaneous solution of Maxwell's relations, and conservation of mass, momentum, and energy for electrons, ions, and neutrals under various initial and boundary conditions, and with suitable simplifying assumptions. Discussions with various experienced authorities on this type of calculation are preceding attempts at formal programming for a computor.

VII. SUMMARY AND PROJECTION

As shown above, a pinch-generating machine is now in operation which is capable of utilizing a significant portion of the electrical energy provided by the capacitor bank to accelerate a single, impermeable current pulse over a $2\frac{1}{2}$ inch radial excursion. Simple modifications to this machine permit the gas thus accelerated to emerge from a central orifice, and this exhaust can be studied by a variety of techniques, most of them well-proven by studies of earlier pinch discharges. Much of the effort in the coming months will be devoted to this class of experiments.

The arrival of the pulse-forming machine described in section V opens the way for a broad variety of studies on discharges driven by prescribed current waveforms. Comparison of their observed behavior under selected external circuit conditions with the appropriate theoretical calculations should help both in the understanding of the details of the acceleration process, and in the formulation of more incisive analytical models.

REFERENCES

1. "Proposed Studies of the Formation and Stability of an Electromagnetic Boundary in a Pinch." Proposal for NASA Research Grant NsG-306-63, 5 March 1962.

2. First Semi-Annual Progress Report for the period 1 July 1962 to 31 December 1962, Research Grant NsG-306-63, Aeronautical Engineering Report No. 634, Princeton University, Princeton, New Jersey.

3. "The Plasma Pinch as a Gas Accelerator," AIAA Electric Propulsion Conference, 11-13 March 1963, preprint 63013.

4. Second Semi-Annual Progress Report for the period 1 January 1963 to 30 June 1963, Research Grant NsG-306-63, Aeronautical Engineering Report No. 634a, Princeton University, Princeton, New Jersey.

5. "Structure of a Large-Radius Pinch Discharge," AIAA Journal 1, 8, 1809 (1963).

6. "Gas-Triggered Inverse Pinch Switch," Review of Scientific Instruments, 34, 12, 1439 (1963).

7. "A Gas-Triggered Inverse Pinch Switch." Technical Note, Aeronautical Engineering Report No. 660, Princeton University, Princeton, New Jersey.

8. "Pulsed Electromagnetic Gas Acceleration," paper No. II, 8, Fourth NASA Intercenter Conference on Plasma Physics in Washington, D. C., 2-4 December 1963.

9. Third Semi-Annual Progress Report for the period 1 July 1963 to 31 December 1963, Research Grant NsG-306-63, Aeronautical Engineering Report No. 634b, Princeton University, Princeton, New Jersey.

10. "Pulsed Electromagnetic Gas Acceleration," a renewal proposal for extension of NASA Research Grant NsG-306-63, Princeton University, Princeton, New Jersey, 15 January 1964.

11. "Current Distributions in Large-Radius Pinch Discharges," AIAA Bulletin 1, 1, 12 (1964).

12. "Current Distributions in Large-Radius Pinch Discharges," AIAA Aerospace Sciences Meeting, New York, New York, 20-22 January 1964, preprint 64-25.

13. "Current Distributions in Large-Radius Pinch Discharges," AIAA Journal 2, (1964).

14. "Gas Triggered Pinch Discharge Switch," The Review of Scientific Instruments 35, (1964).

15. "Gas Triggered Pinch Discharge Switch," Princeton Technical Note No. 101, Princeton University, Princeton, New Jersey, July 1964.

Appendix I: Pulse-forming Network Calculations

As one example of the type of computation necessary to design the pulse-forming experiment, consider the transient response of an equi-section L-C ladder network, including the effect of the self-inductance of the capacitors. The circuit may be represented schematically as sketched,

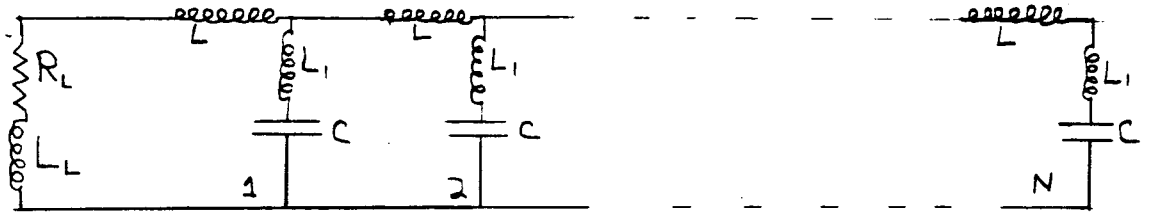

and specified analytically by the six parameters: R_L, L_L, L, L_1, C, and N, where the discharge has been approximated as a series inductance-resistance load, R_L and L_L, and N is the number of sections. Suitable nondimensionalization can reduce the number of characteristic parameters to four. Mathematically, a "brute-force" approach was most suitable for machine computation: the N second order loop equations are cast into 2N first order equations with suitable initial conditions, and integrated numerically on an IBM 7094. Fig. (24) displays typical solutions, and shows the effect of increasing the number of sections in the network.

In a related calculation, a five loop network was programmed to permit arbitrary capacitance and inductance values in each section. Fig. (25) shows a resulting equi-section five loop wave-form, and displays the drastic effects of reducing the first loop inductance to zero.

At present a program is being prepared to yield the response of an L-C ladder network having both the component values and the number of sections as variables of the problem, corresponding to the experimental flexibility of the new pulse-driven apparatus.

A variational approach to the problem of circuit optimization is also under investigation. This attack is mathematically straightforward, but the amount of computation is large and increases somewhat faster than the square of the number of sections.

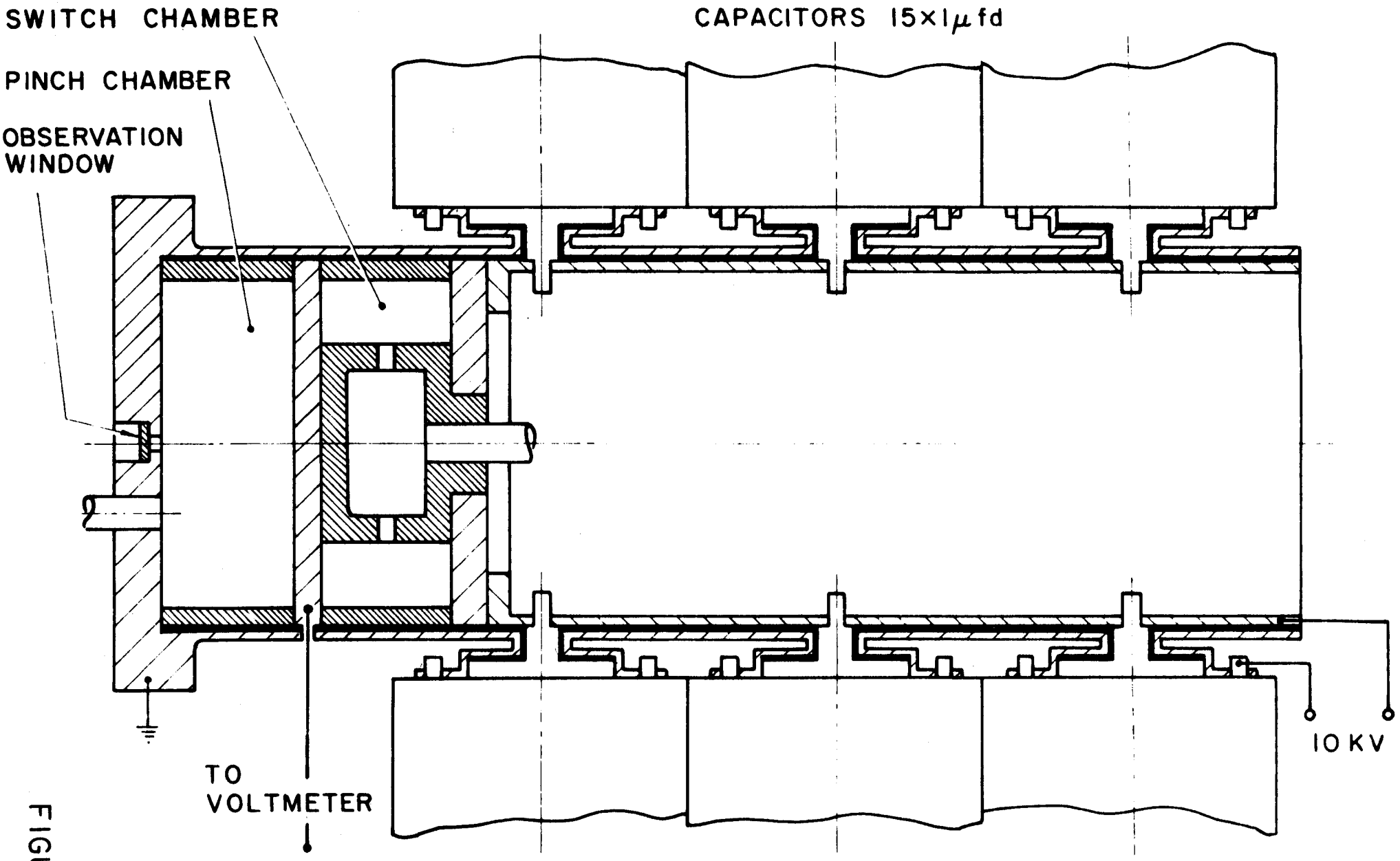

FIGURE 1

5" PLASMA PINCH APPARATUS (SCHEMATIC)

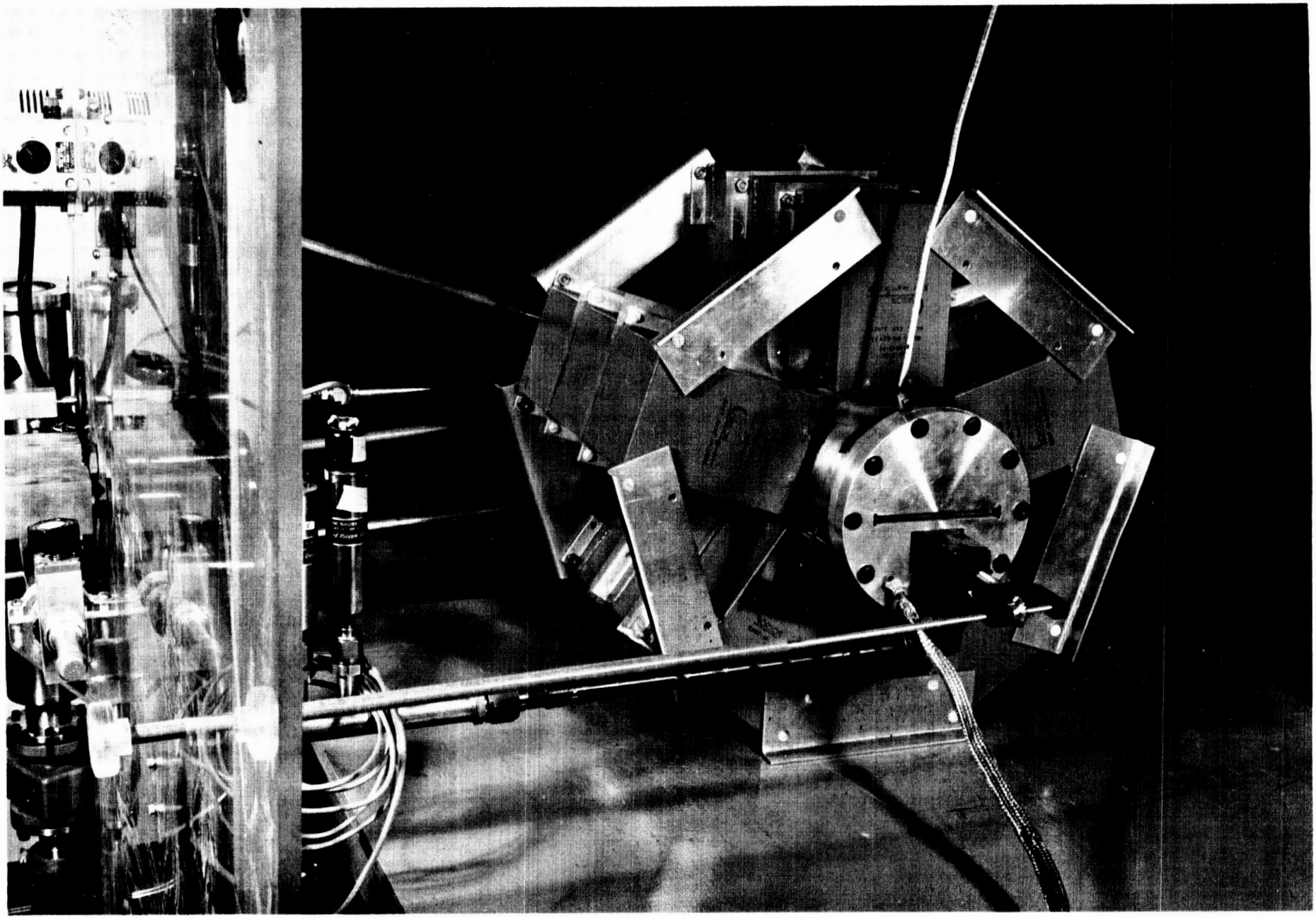

VIEW OF TUBULAR PLASMA PINCH APPARATUS

FIGURE 2

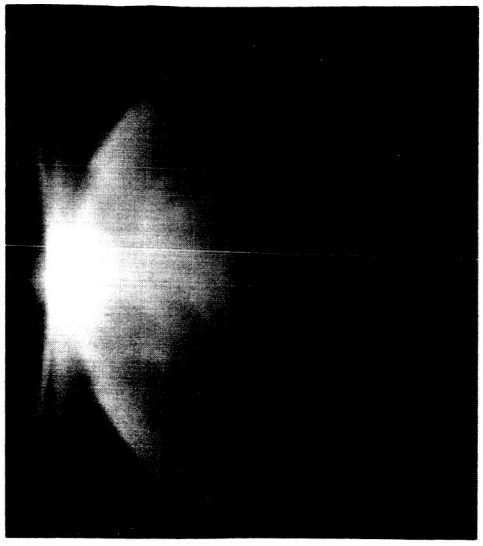

0 4 8 12 μ sec

53 μ ARGON – 5"

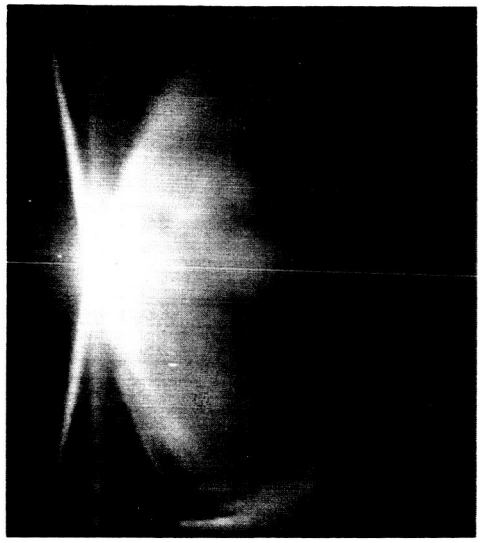

0 4 8 12 μ sec

138 μ ARGON – 5"

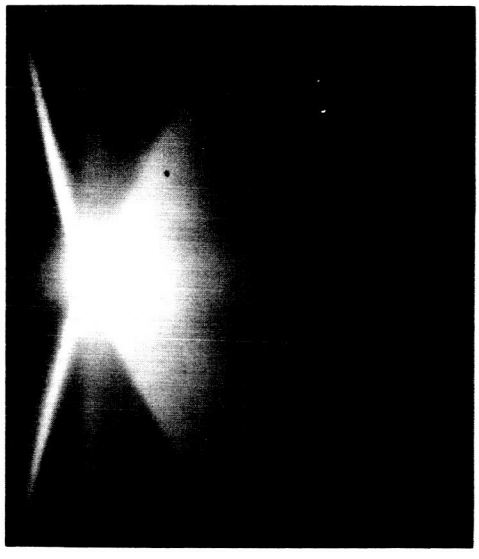

0 4 8 12 μ sec

275 μ ARGON – 5"

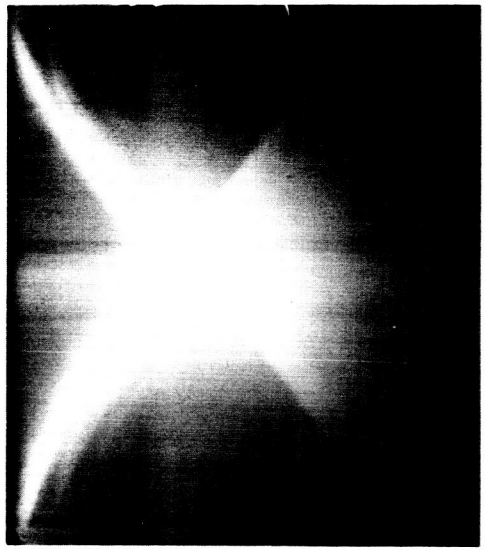

0 4 8 12 μ sec

1550 μ ARGON – 5"

STREAK PHOTOGRAPHS OF PINCH DISCHARGE IN ARGON – 5" TUBULAR MACHINE

FIGURE 3

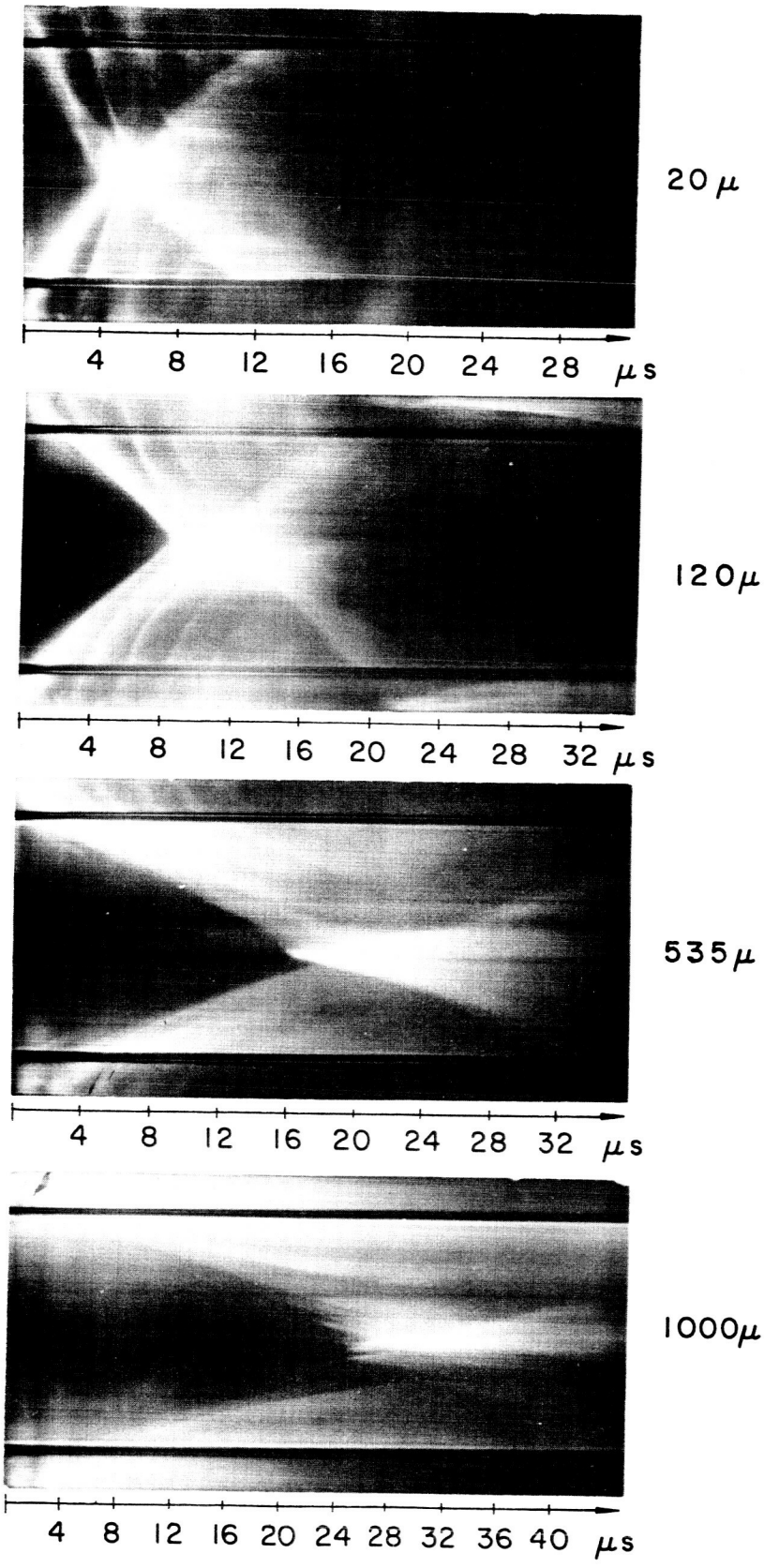

STREAK PHOTOGRAPHS OF PINCH DISCHARGE IN ARGON - 8" MACHINE

FIGURE 4

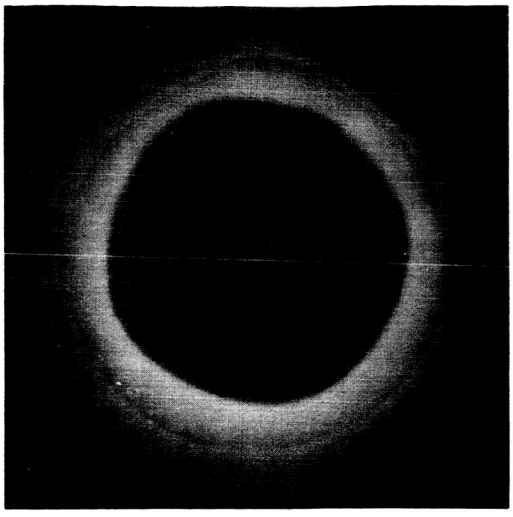

3.0 μs

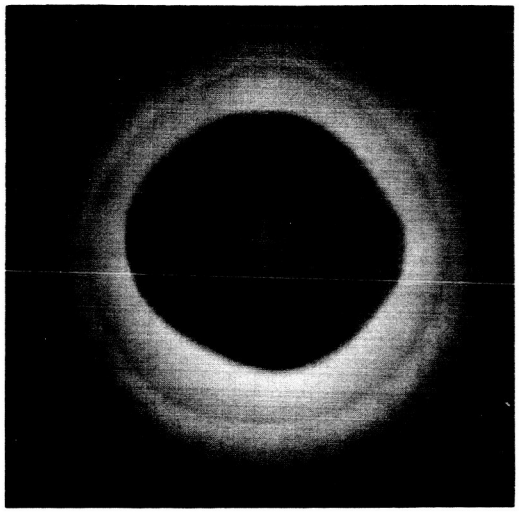

3.5 μs

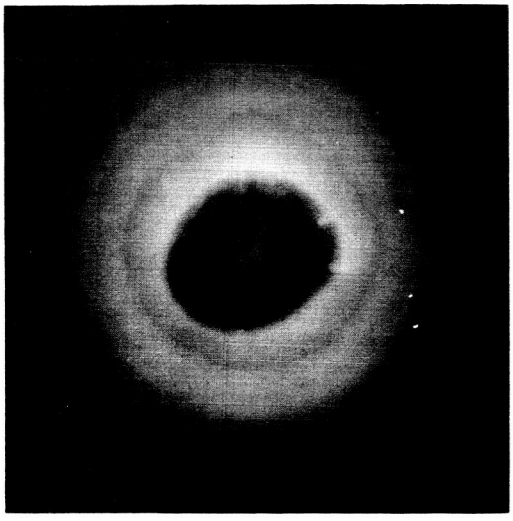

4.3 μs

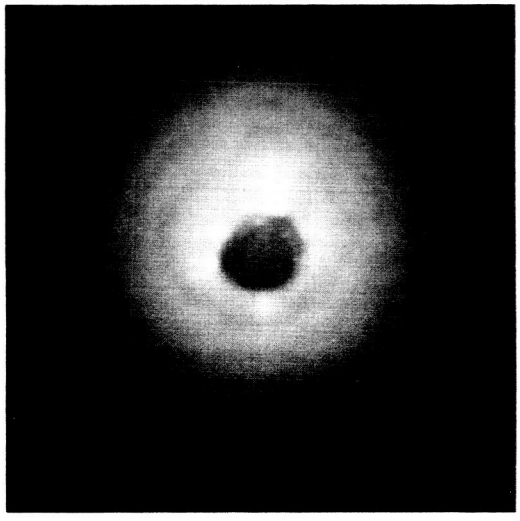

4.9 μs

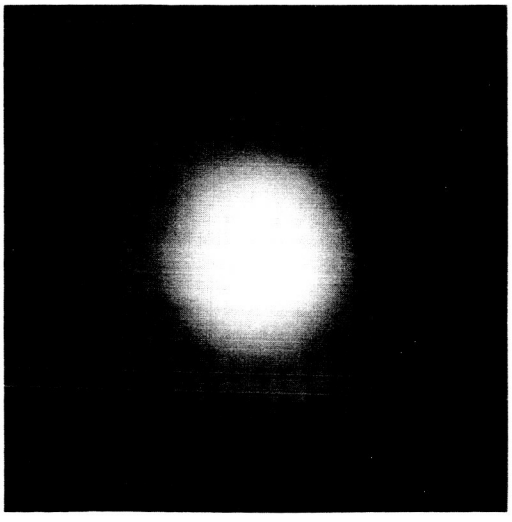

6.7 μs

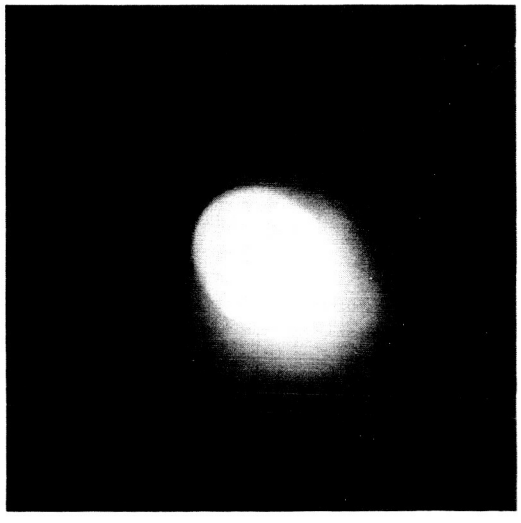

7.7 μs

AXIAL PHOTOGRAPHS OF 5" PINCH DISCHARGE
1920 μ ARGON; 0.05 μs EXPOSURE

FIGURE 5

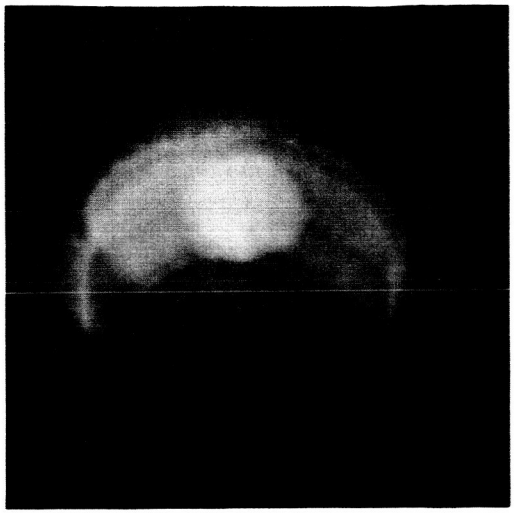

2.7 μs

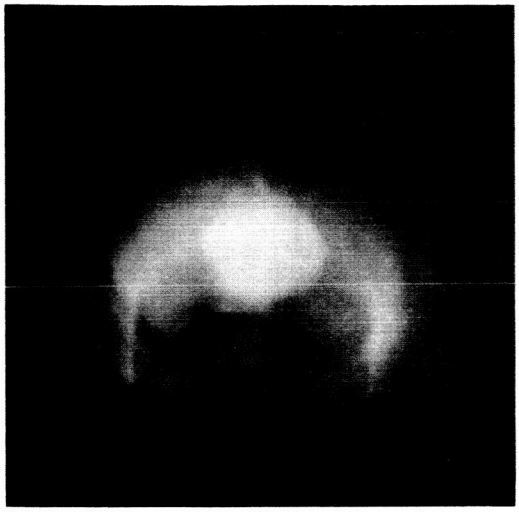

3.2 μs

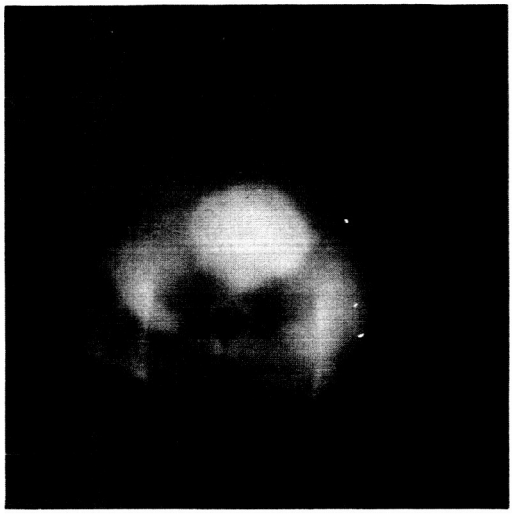

3.8 μs

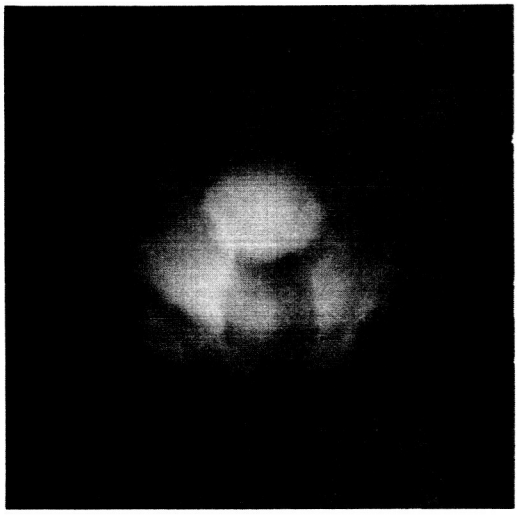

4.8 μs

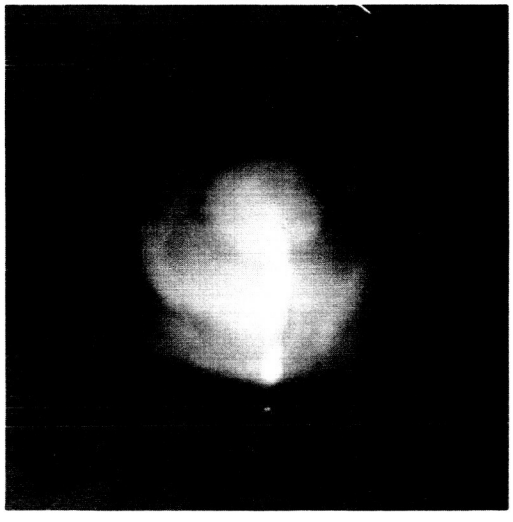

5.0 μs

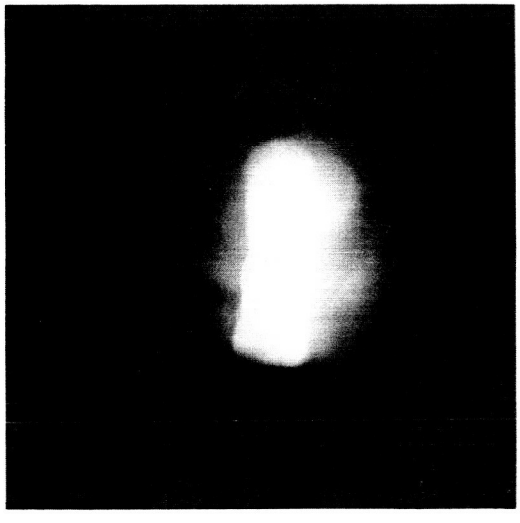

6.8 μs

PERSPECTIVE PHOTOGRAPHS OF 5" PINCH DISCHARGE
1920 μ ARGON ; 0.05 μs EXPOSURE

FIGURE 6

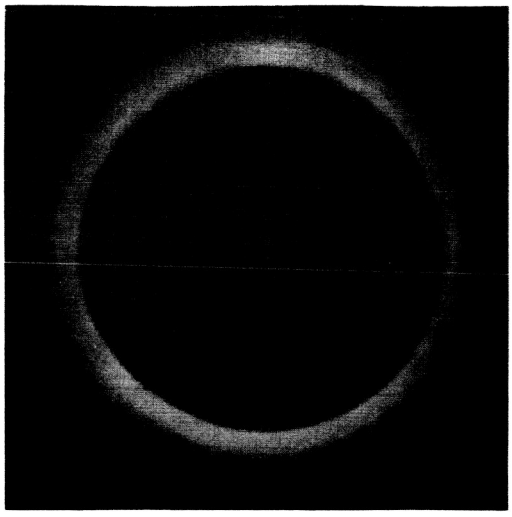

1.4 μs

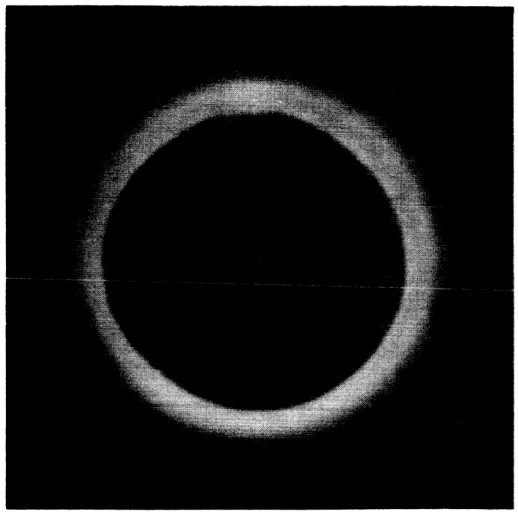

1.6 μs

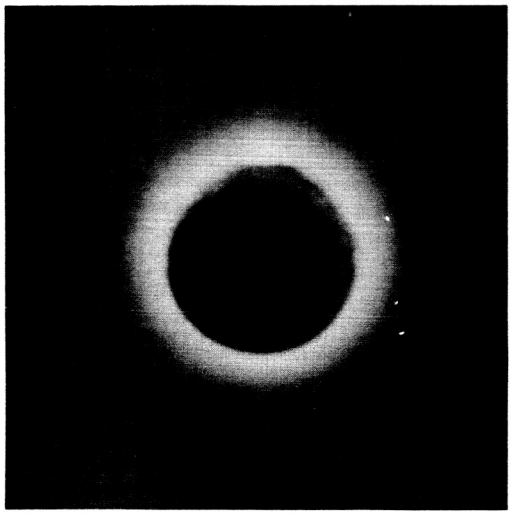

2.1 μs

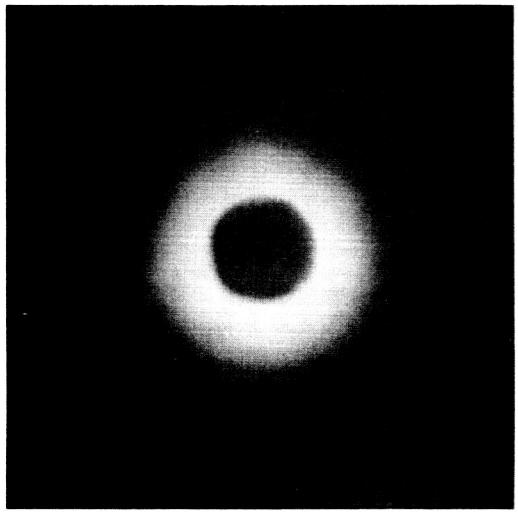

2.7 μs

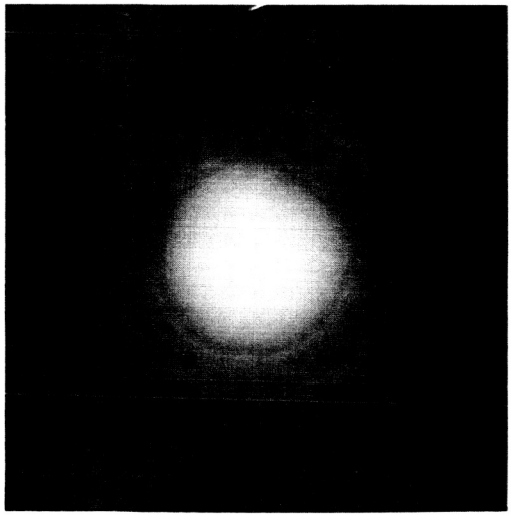

3.1 μs

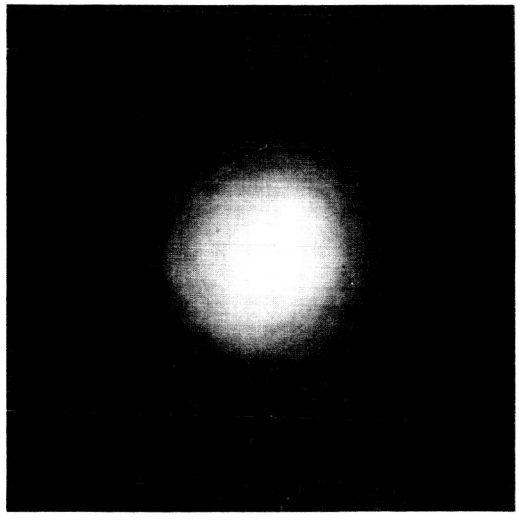

3.5 μs

AXIAL PHOTOGRAPHS OF 5" PINCH DISCHARGE
480 μ ARGON ; 0.05 μs EXPOSURE

FIGURE 7

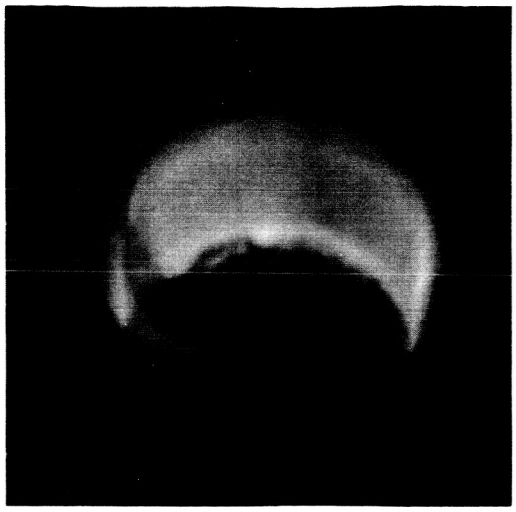

1.2 μs

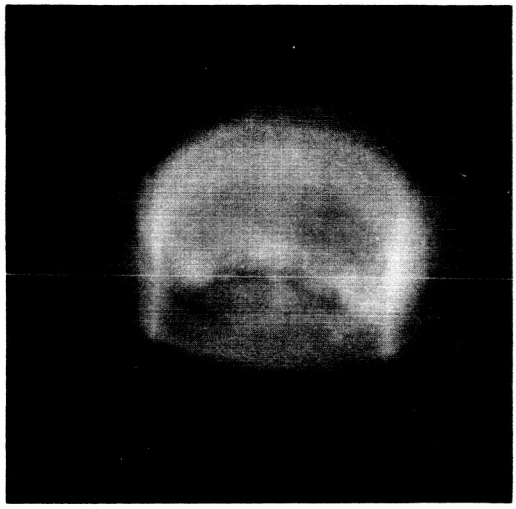

2.1 μs

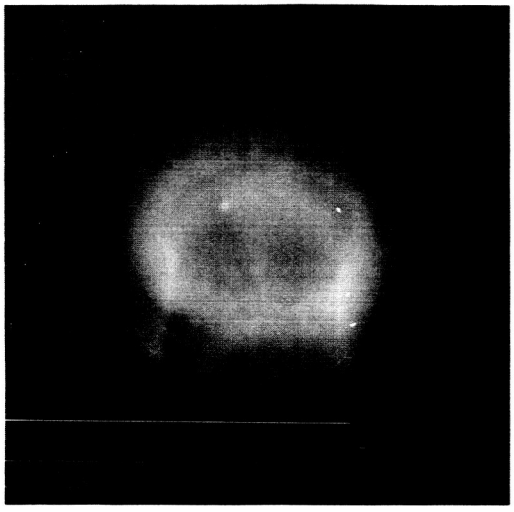

2.4 μs

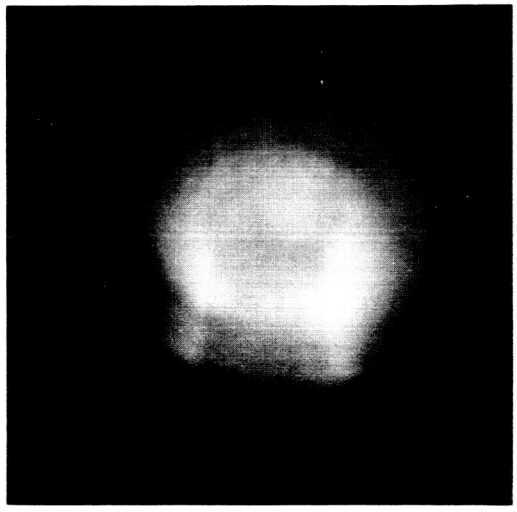

2.5 μs

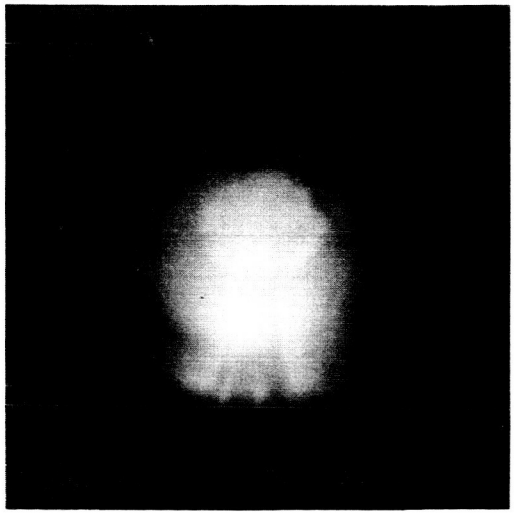

2.7 μs

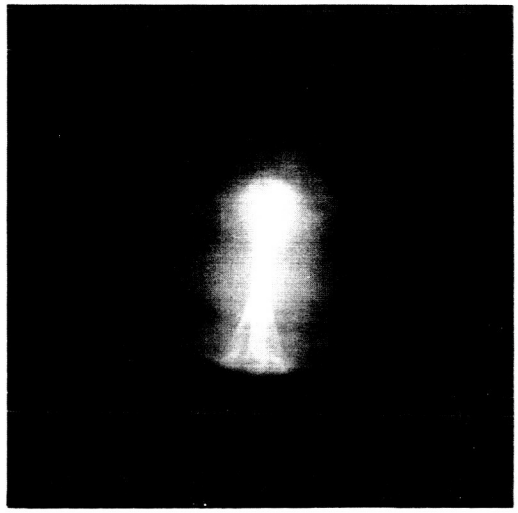

3.0 μs

PERSPECTIVE PHOTOGRAPHS OF 5" PINCH DISCHARGE
480 μ ARGON ; 0.05 μs EXPOSURE

FIGURE 8

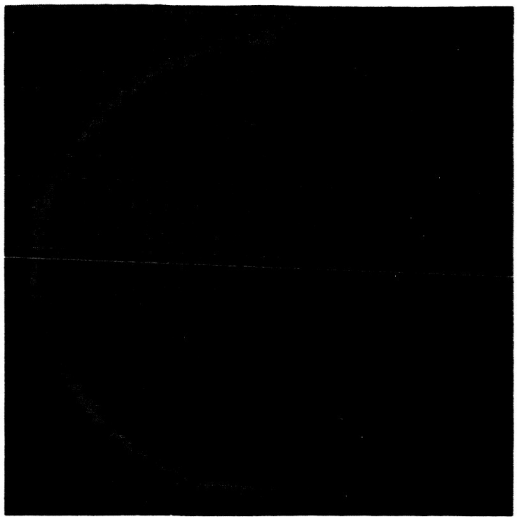

0.8 μs

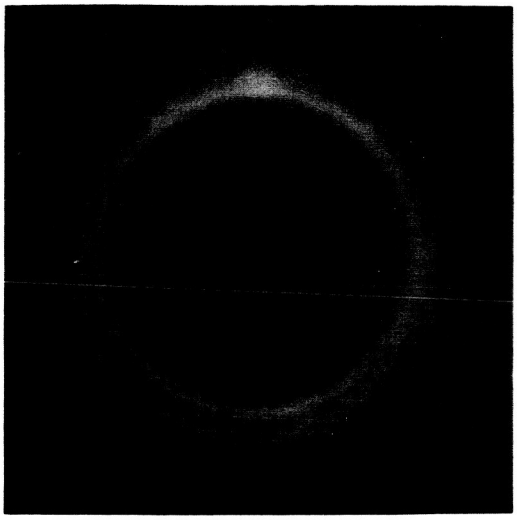

1.0 μs

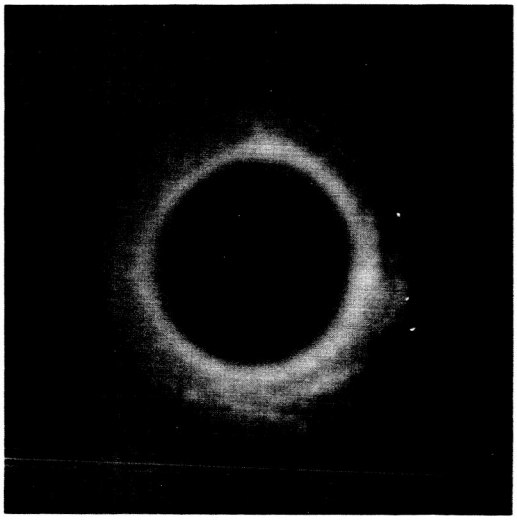

1.3 μs

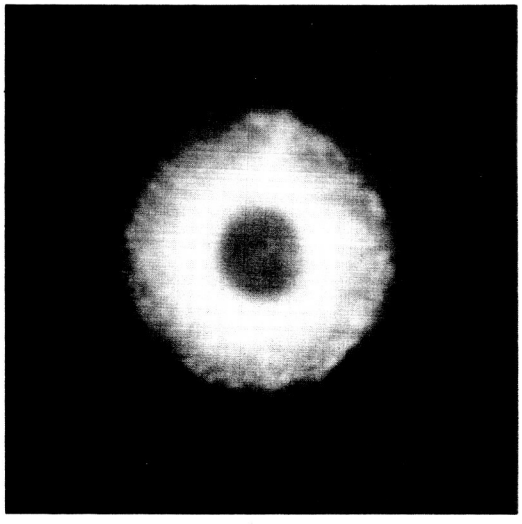

1.4 μs

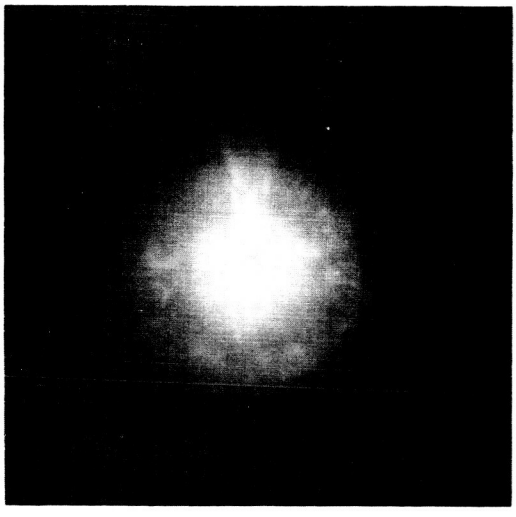

1.6 μs

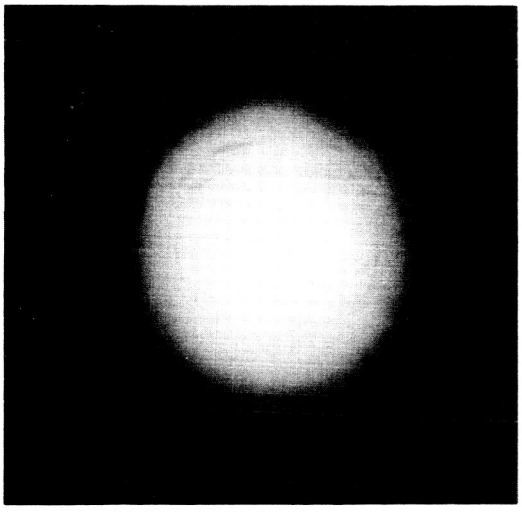

1.7 μs

AXIAL PHOTOGRAPHS OF 5" PINCH DISCHARGE
120 μ ARGON ; 0.05 μs EXPOSURE

FIGURE 9

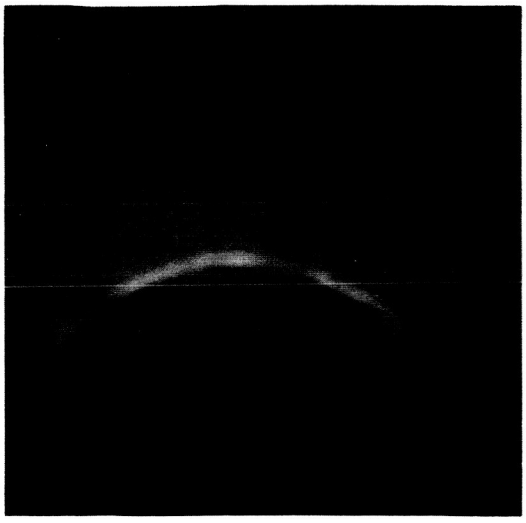

0.8 μs

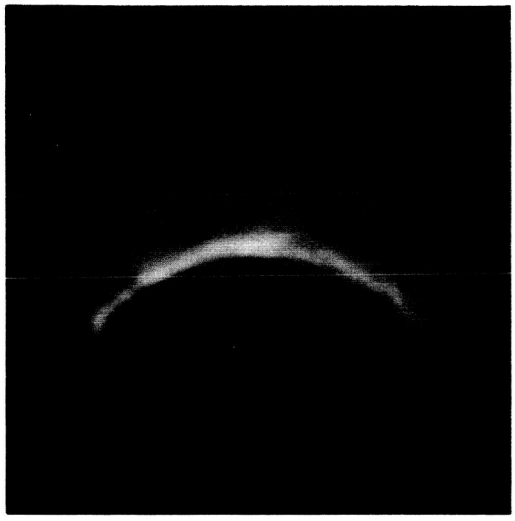

1.0 μs

1.2 μs

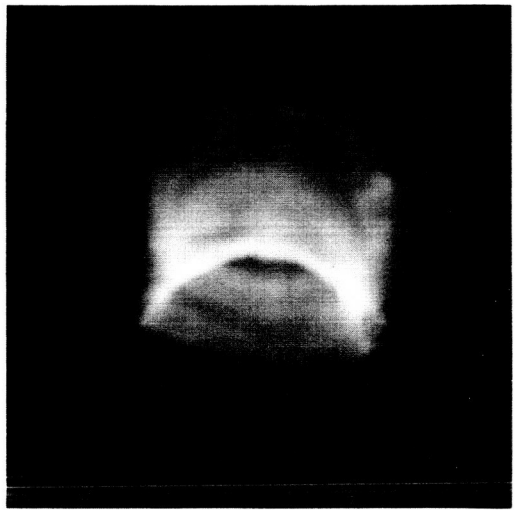

1.3 μs

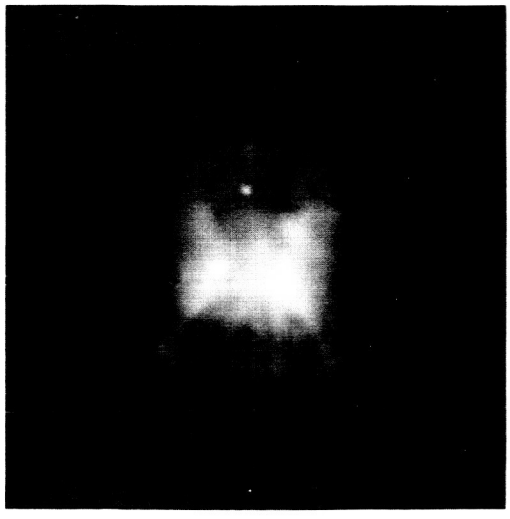

1.5 μs

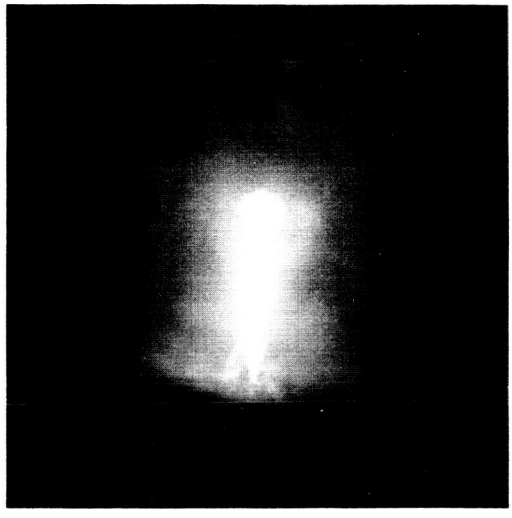

1.9 μs

PERSPECTIVE PHOTOGRAPHS OF 5" PINCH DISCHARGE
120 μ ARGON ; 0.05 μs EXPOSURE

FIGURE 10

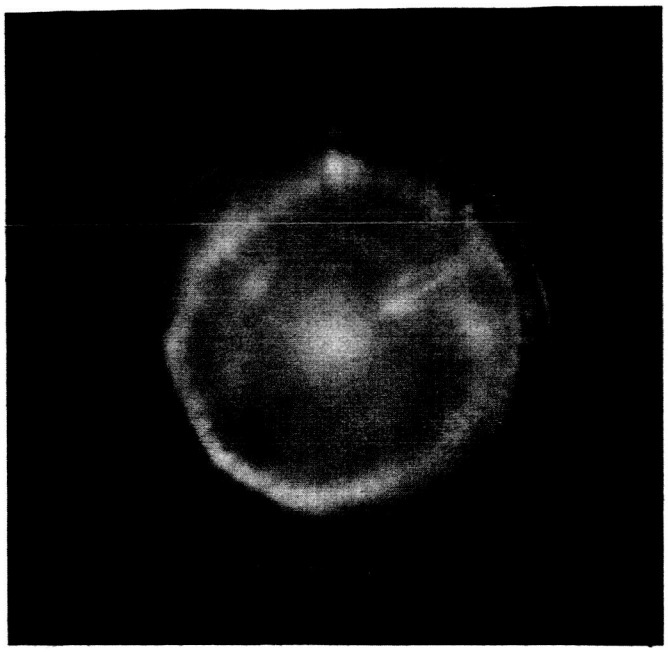

0.8 μs

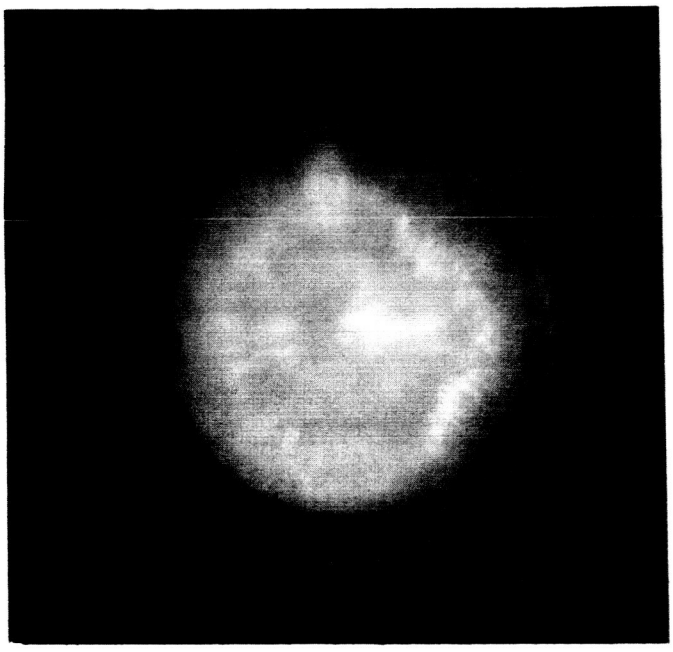

1.0 μs

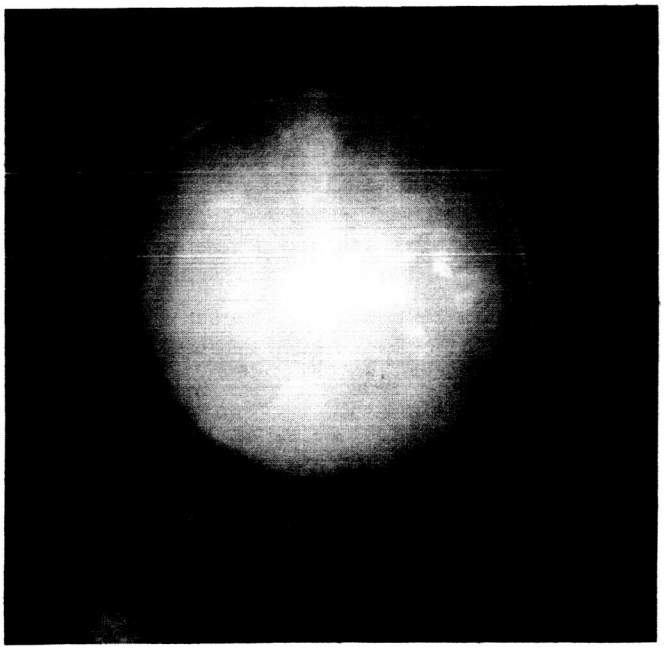

1.1 μs

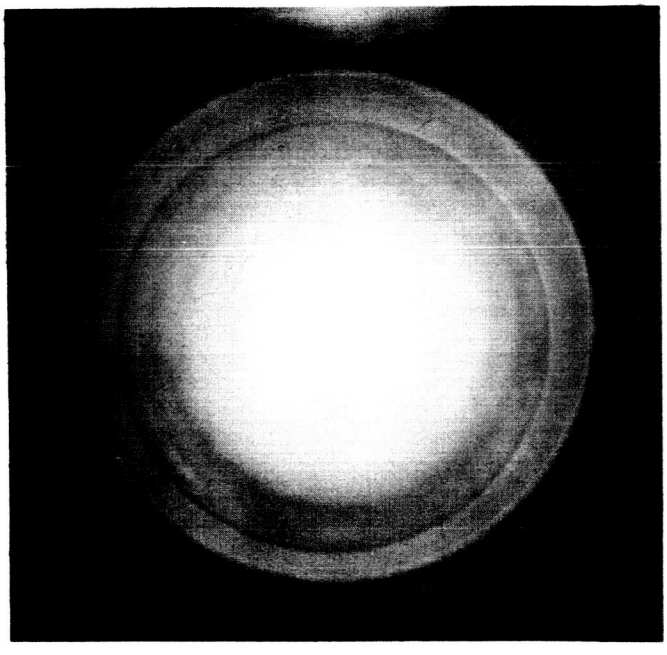

1.2 μs

AXIAL PHOTOGRAPHS OF 5" PINCH DISCHARGE
30 μ ARGON ; 0.05 μs EXPOSURE

FIGURE 11

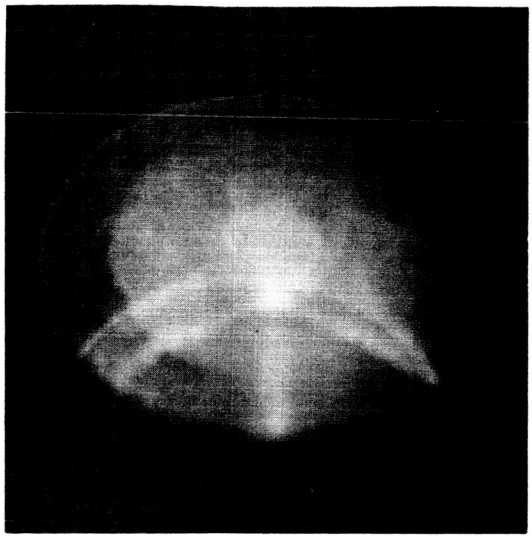

0.7 μs

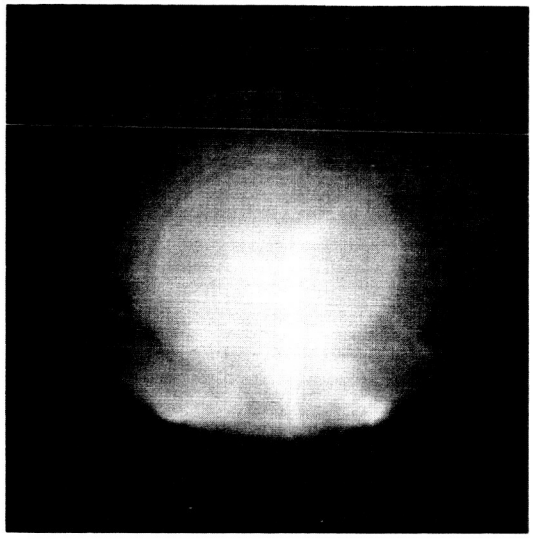

1.0 μs

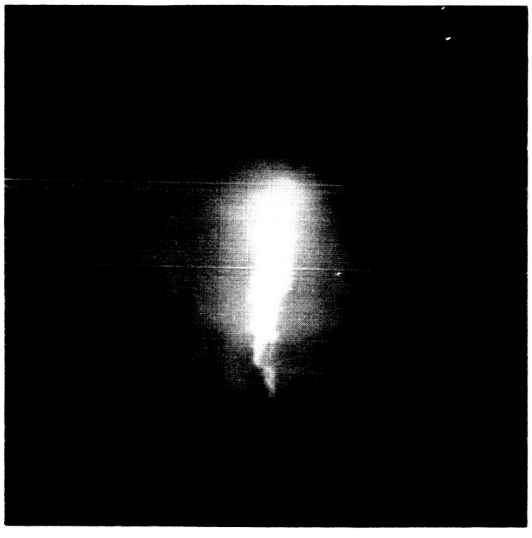

1.0 μs

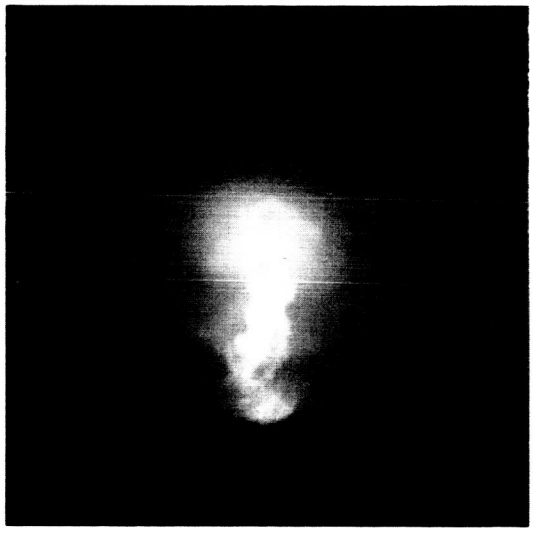

1.2 μs

PERSPECTIVE PHOTOGRAPHS OF 5" PINCH DISCHARGE
30 μ ARGON ; 0.05 μs EXPOSURE

FIGURE 12

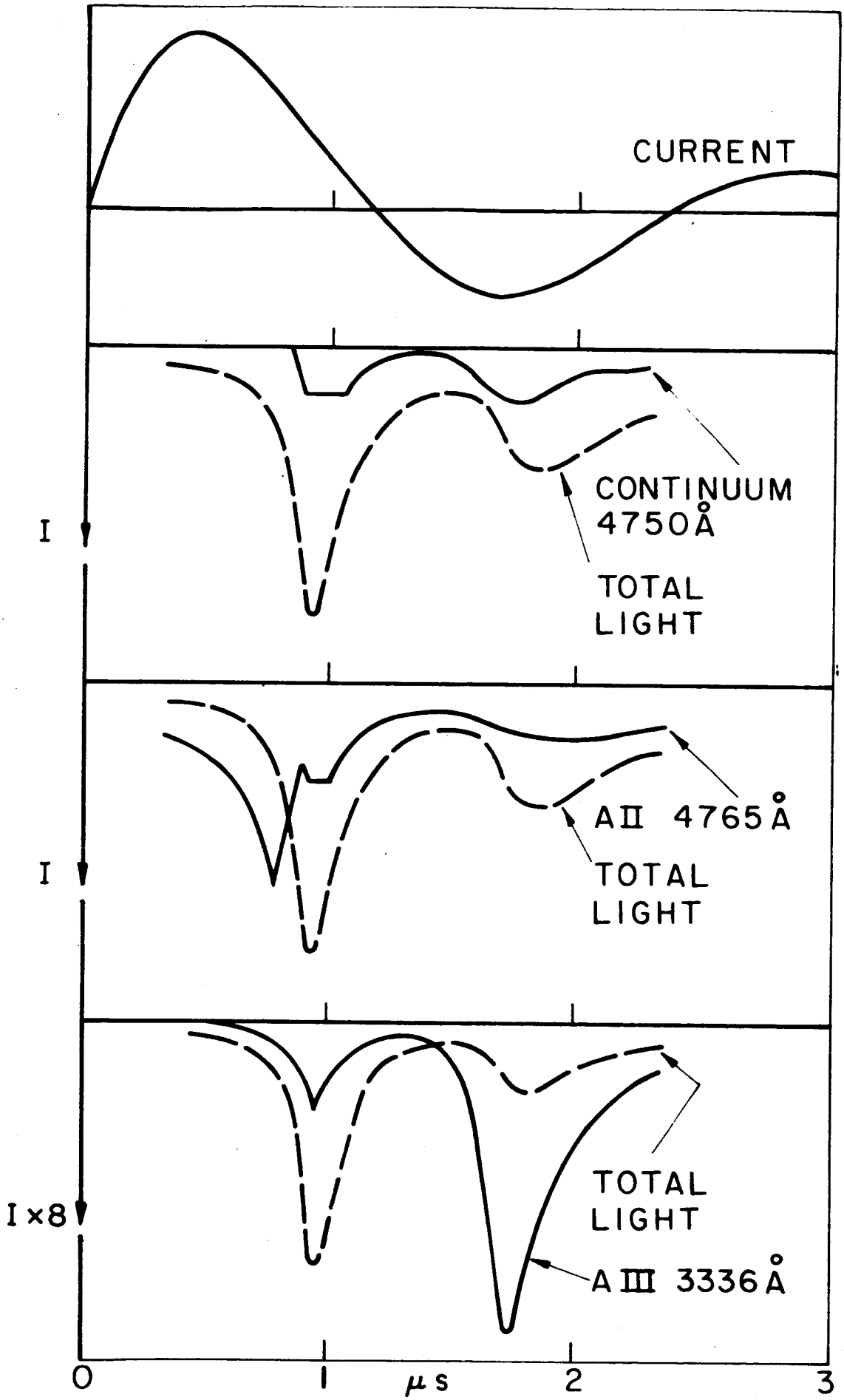

FIG. 13

5" DISCHARGE IN 120 μ ARGON AT $R/R_0 = 1/2$

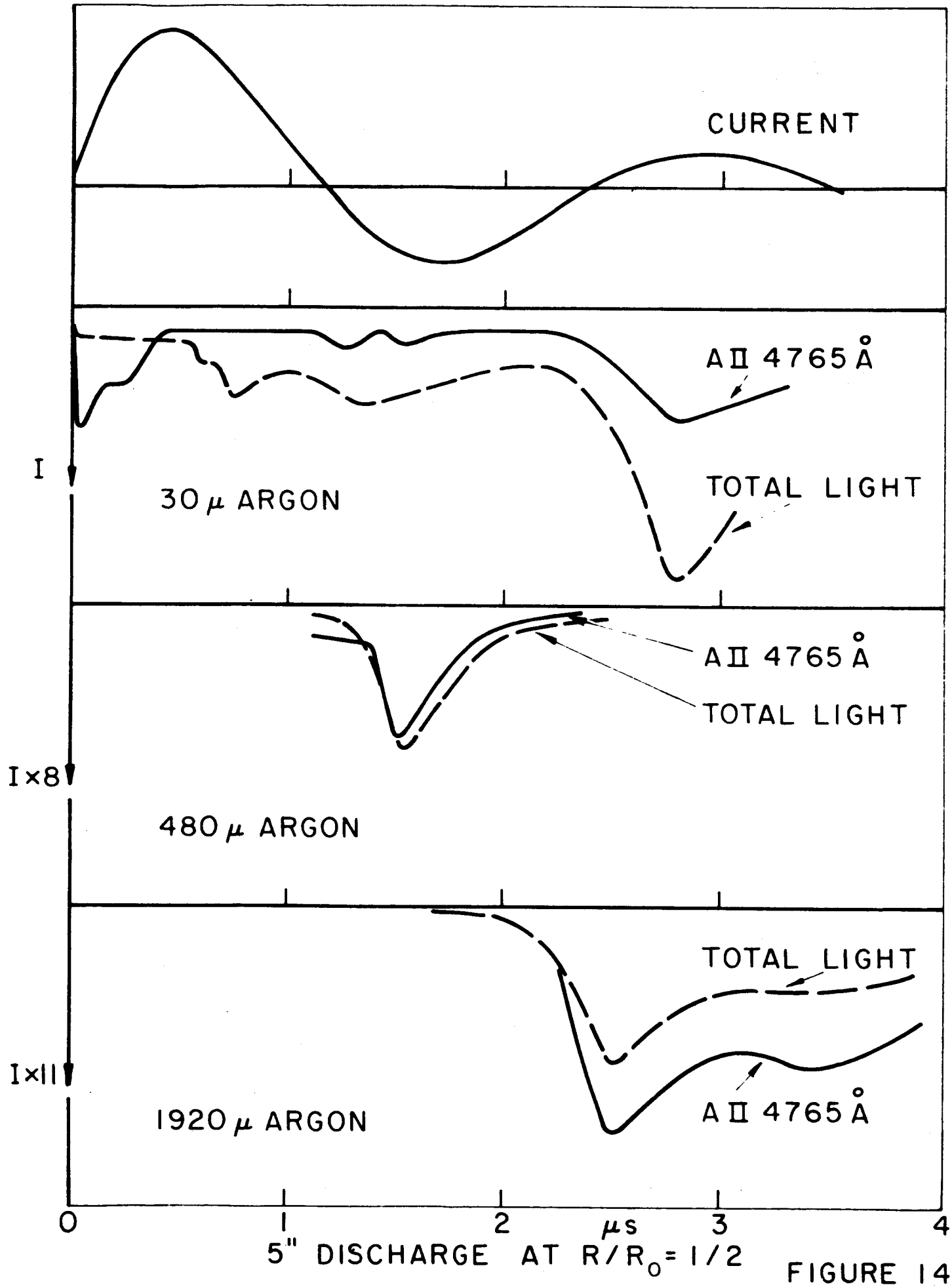
CURRENT
AII 4765 Å
I
30 μ ARGON
TOTAL LIGHT
AII 4765 Å
TOTAL LIGHT
I×8
480 μ ARGON
TOTAL LIGHT
I×11
1920 μ ARGON
AII 4765 Å
0
1
2
μs
3
4
5" DISCHARGE AT R/R0 = 1/2

FIGURE 14

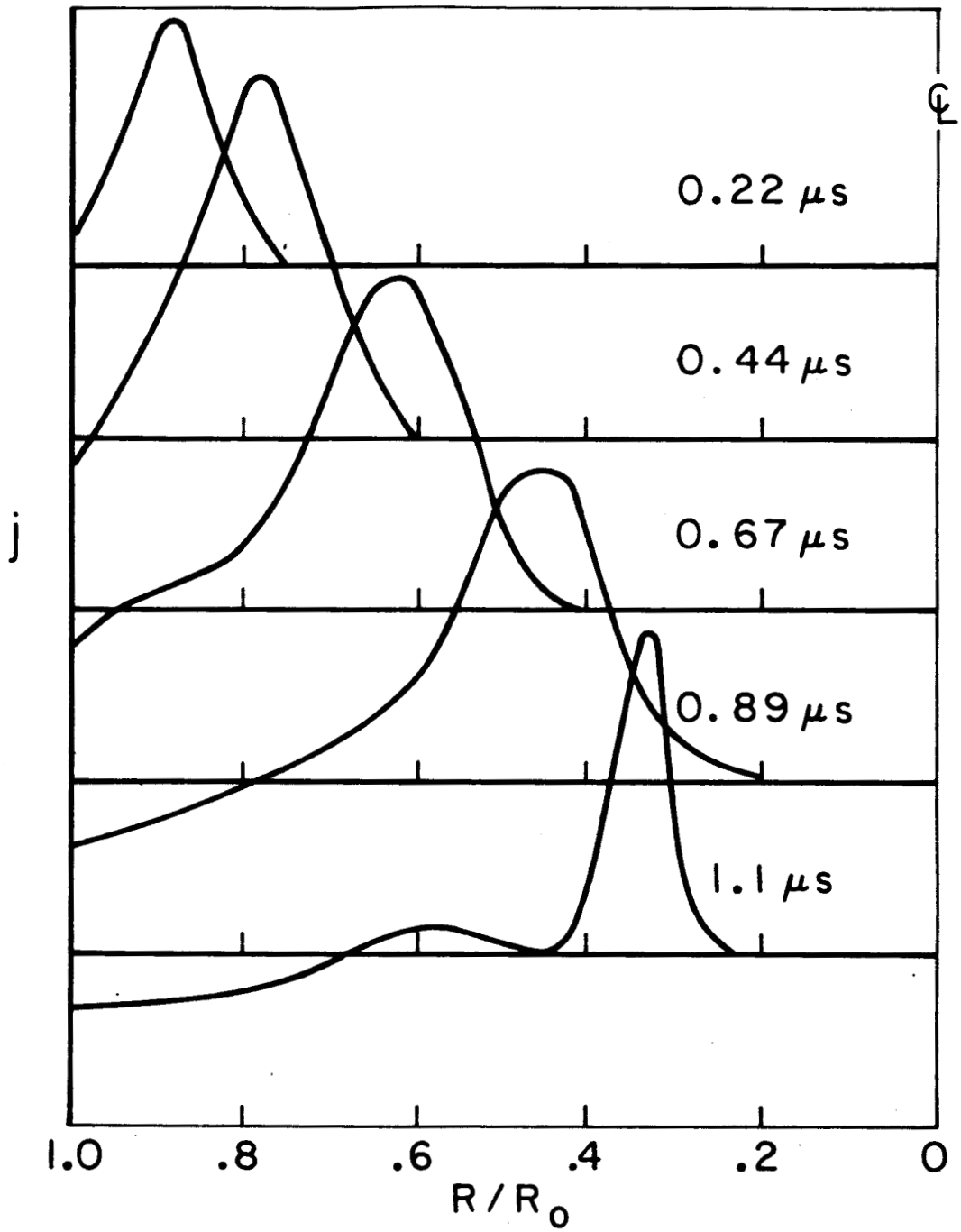

CURRENT DISTRIBUTIONS IN 5" PINCH DISCHARGE IN 120 μ ARGON

FIGURE 15

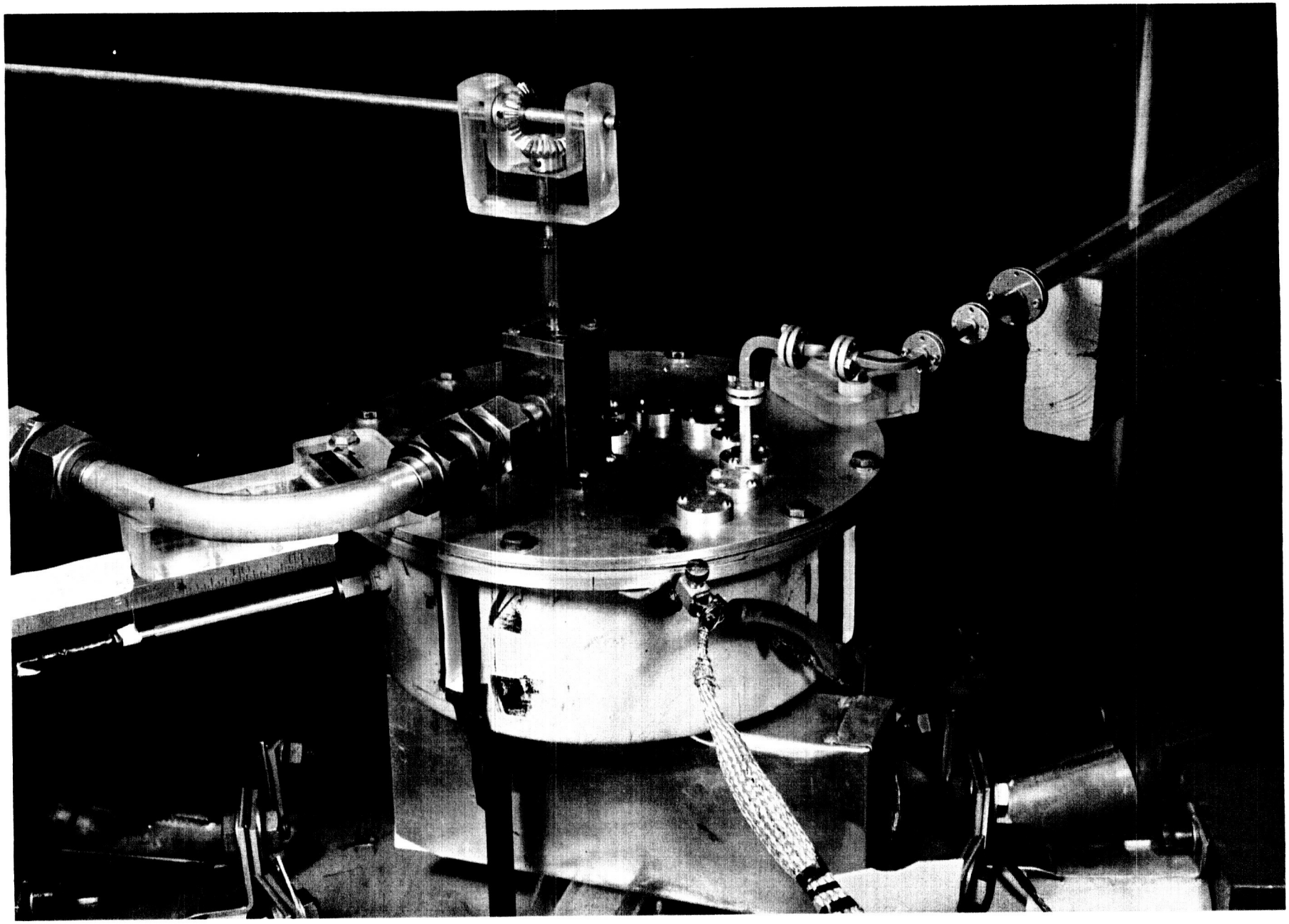

8" PLASMA PINCH CHAMBER WITH ELECTRODE
FOR μ WAVE PROBING

FIGURE 16

D.O.

ARGON

$R / R_0 = .875$

$P = 30\,\mu$

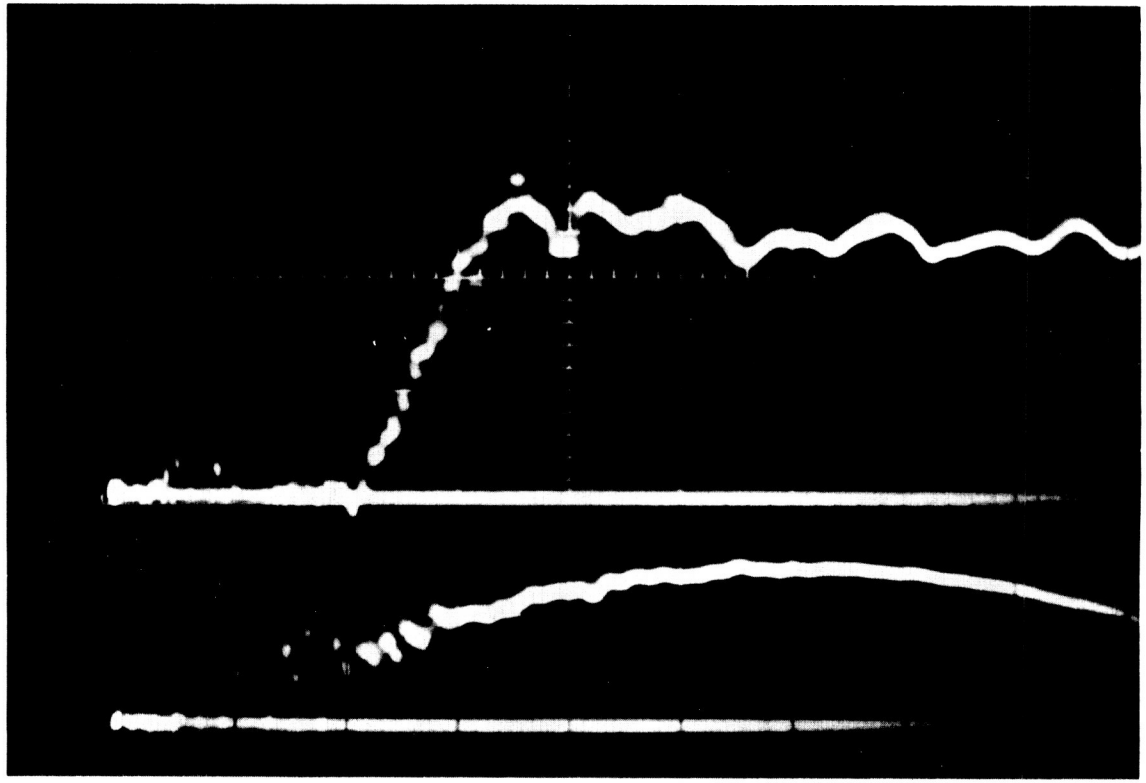

.2 μ sec / cm

UPPER: RESPONSE OF 70 GC MICROWAVE PROBE IN 8" PINCH DISCHARGE

LOWER: CURRENT IN SAME

FIGURE 17

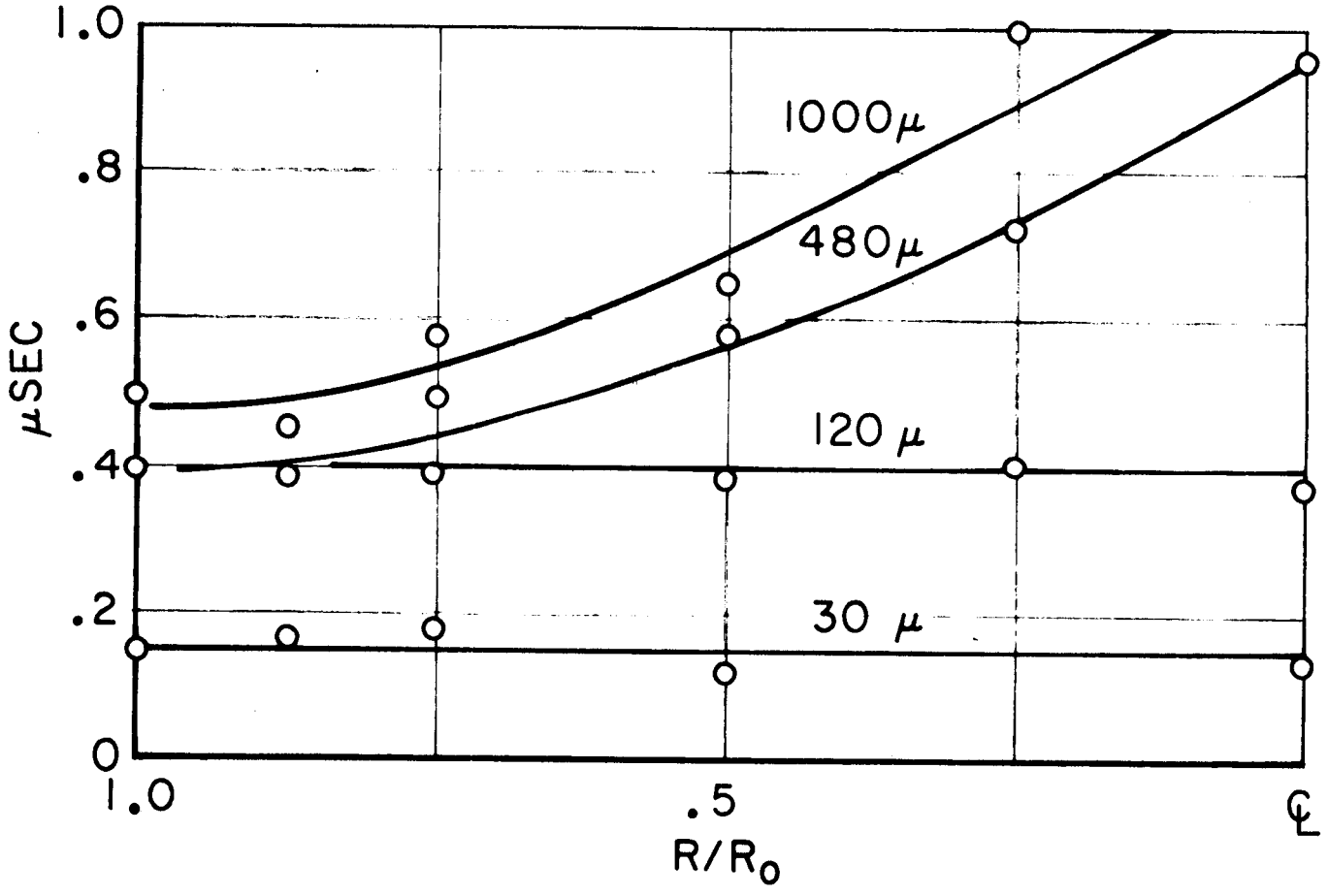

8" PINCH DISCHARGE IN ARGON:
TIME TO 1/2 MAX REFLECTION OF 70 GC

FIGURE 18

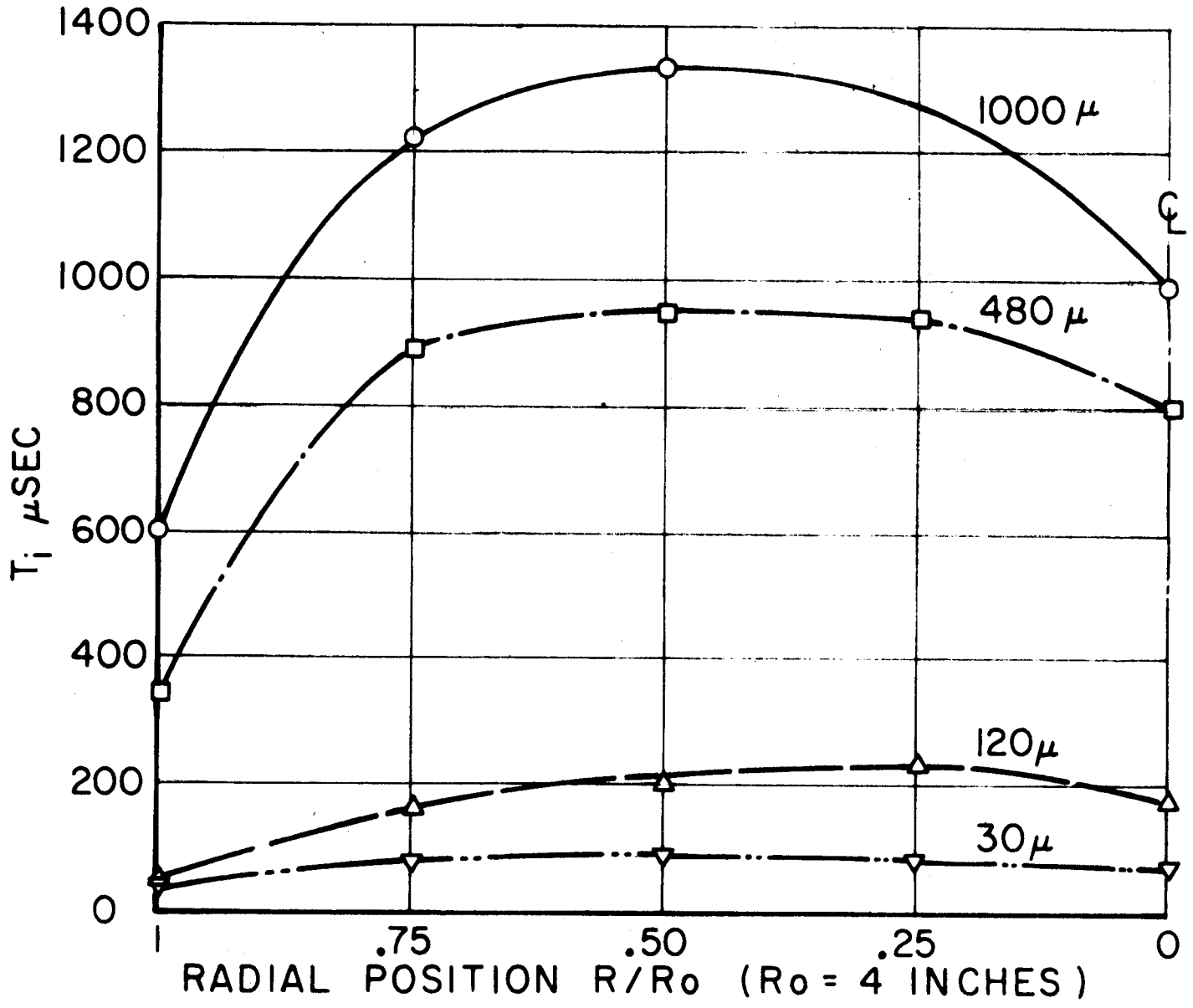

8" PINCH DISCHARGE IN ARGON:
IONIZATION TIME vs RADIAL POSITION, 70GC

FIGURE 19

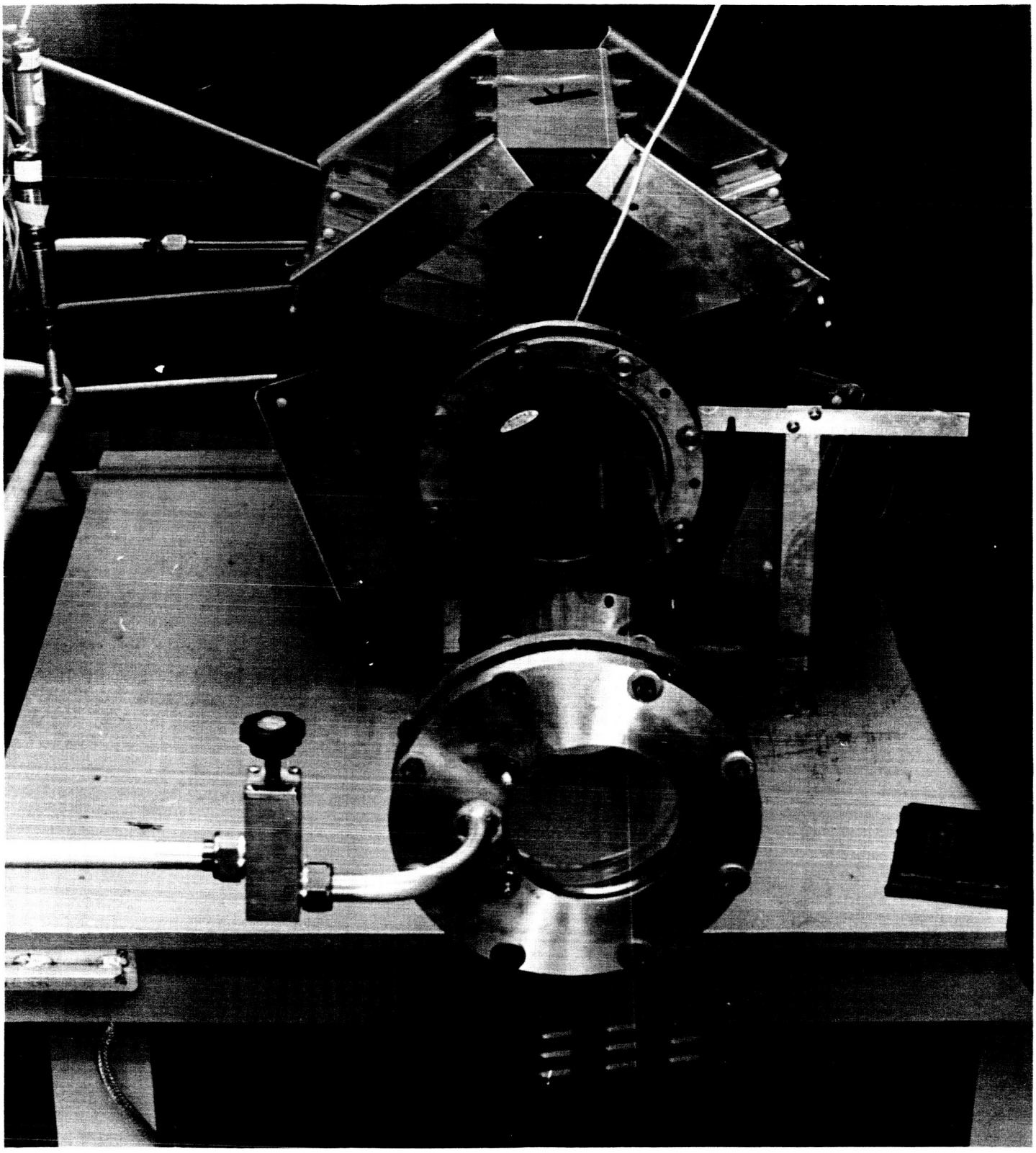

VIEW OF TUBULAR PINCH DISCHARGE APPARATUS
WITH EXIT ORIFICE AND EXHAUST CHAMBER

FIGURE 20

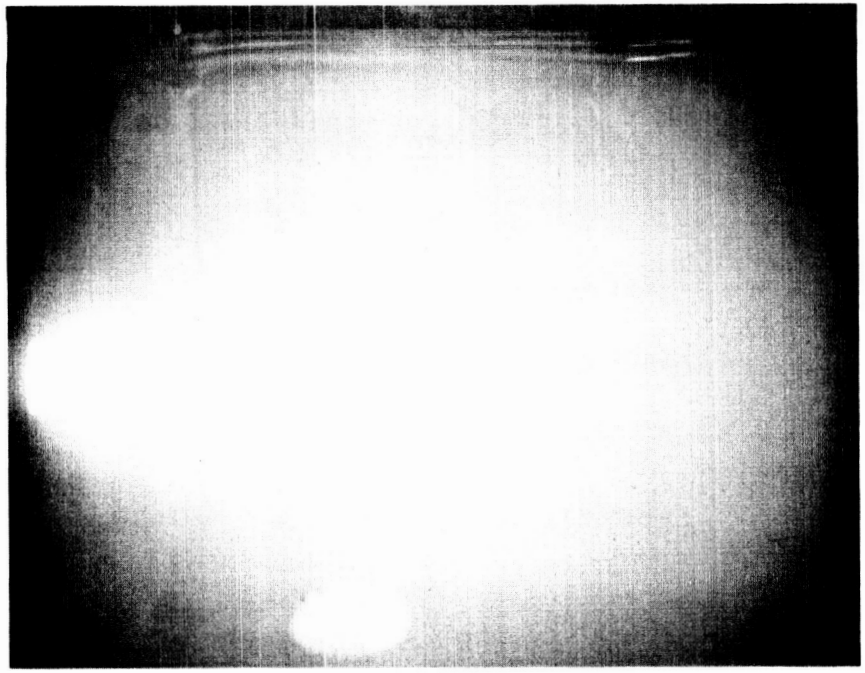

PHOTOGRAPH OF EXHAUST FROM 5" PINCH DISCHARGE IN 120μ ARGON

FIGURE 21

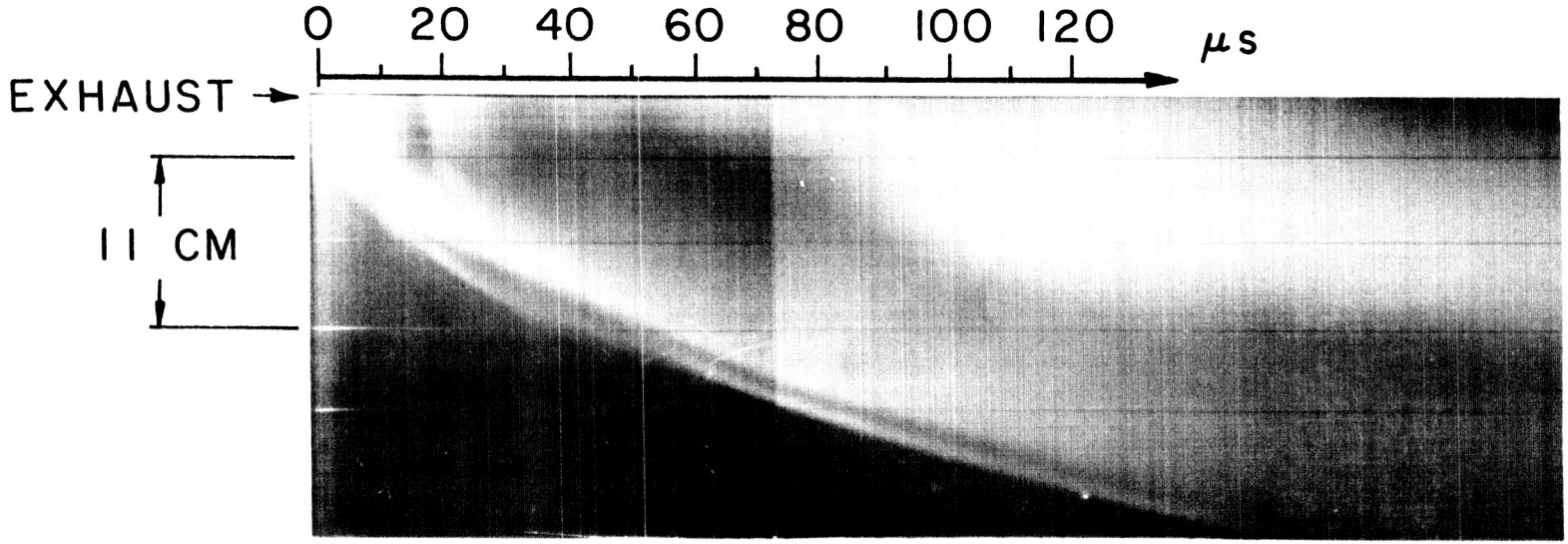

STREAK PHOTOGRAPH OF EXHAUST FROM 5" PINCH DISCHARGE IN 120μ ARGON

FIGURE 22

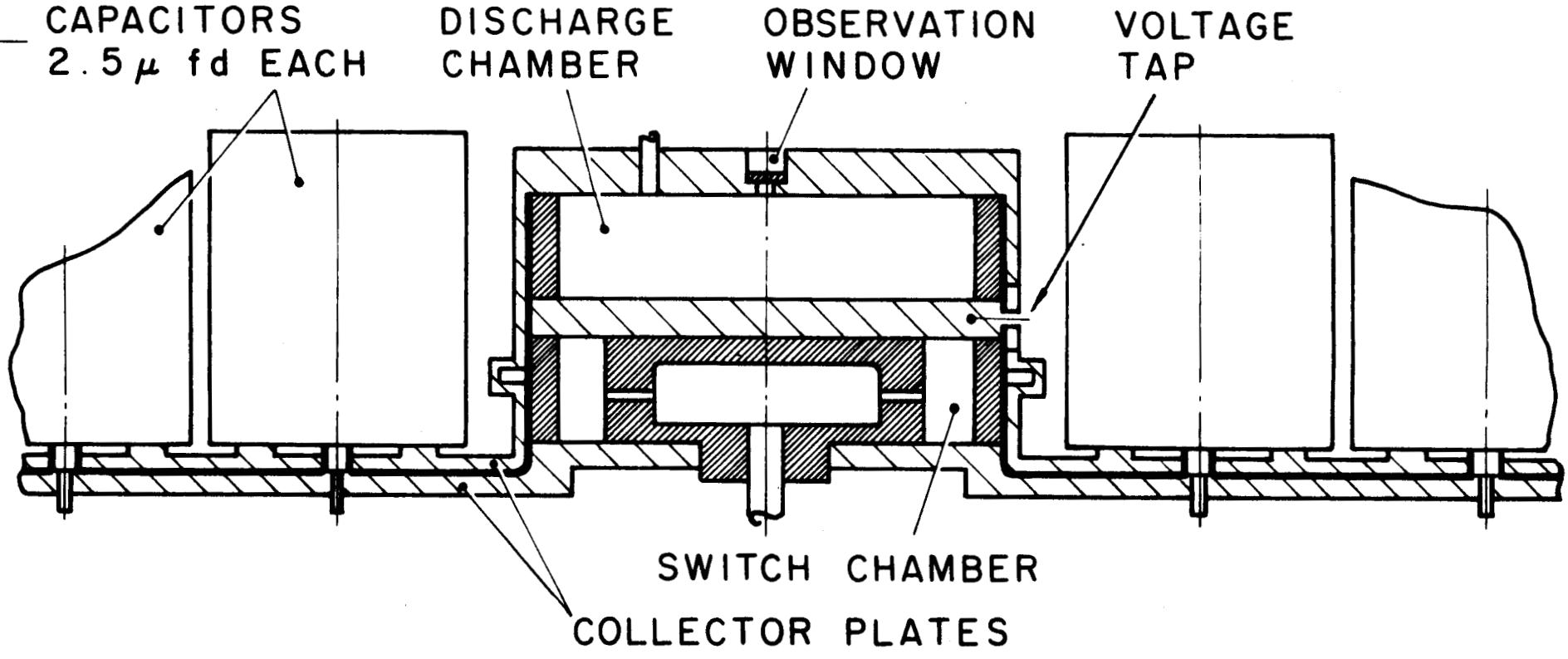

PULSE FORMING PLASMA PINCH APPARATUS (SCHEMATIC)

FIGURE 23

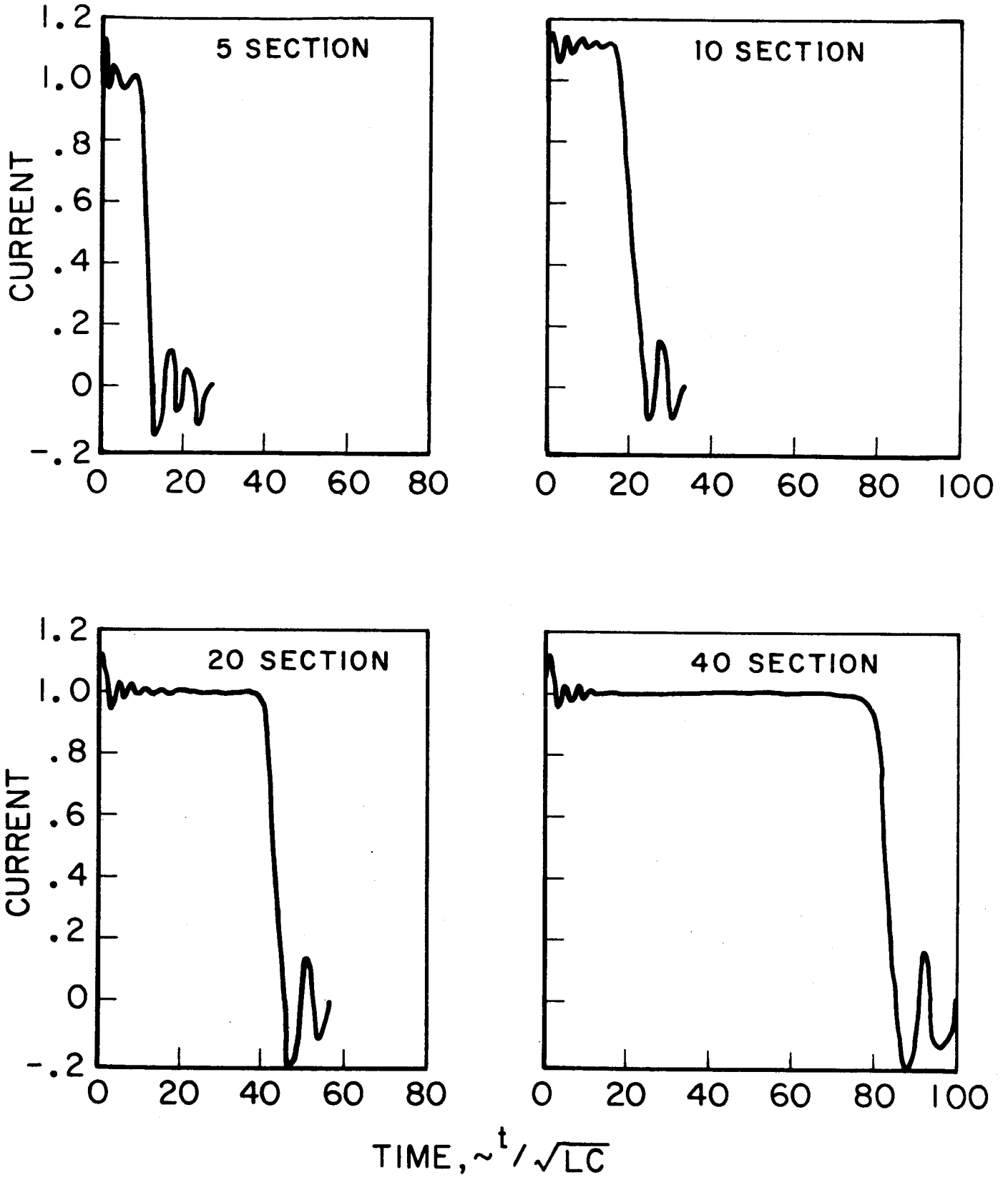

EQUAL- SECTION LINES

FIGURE 24

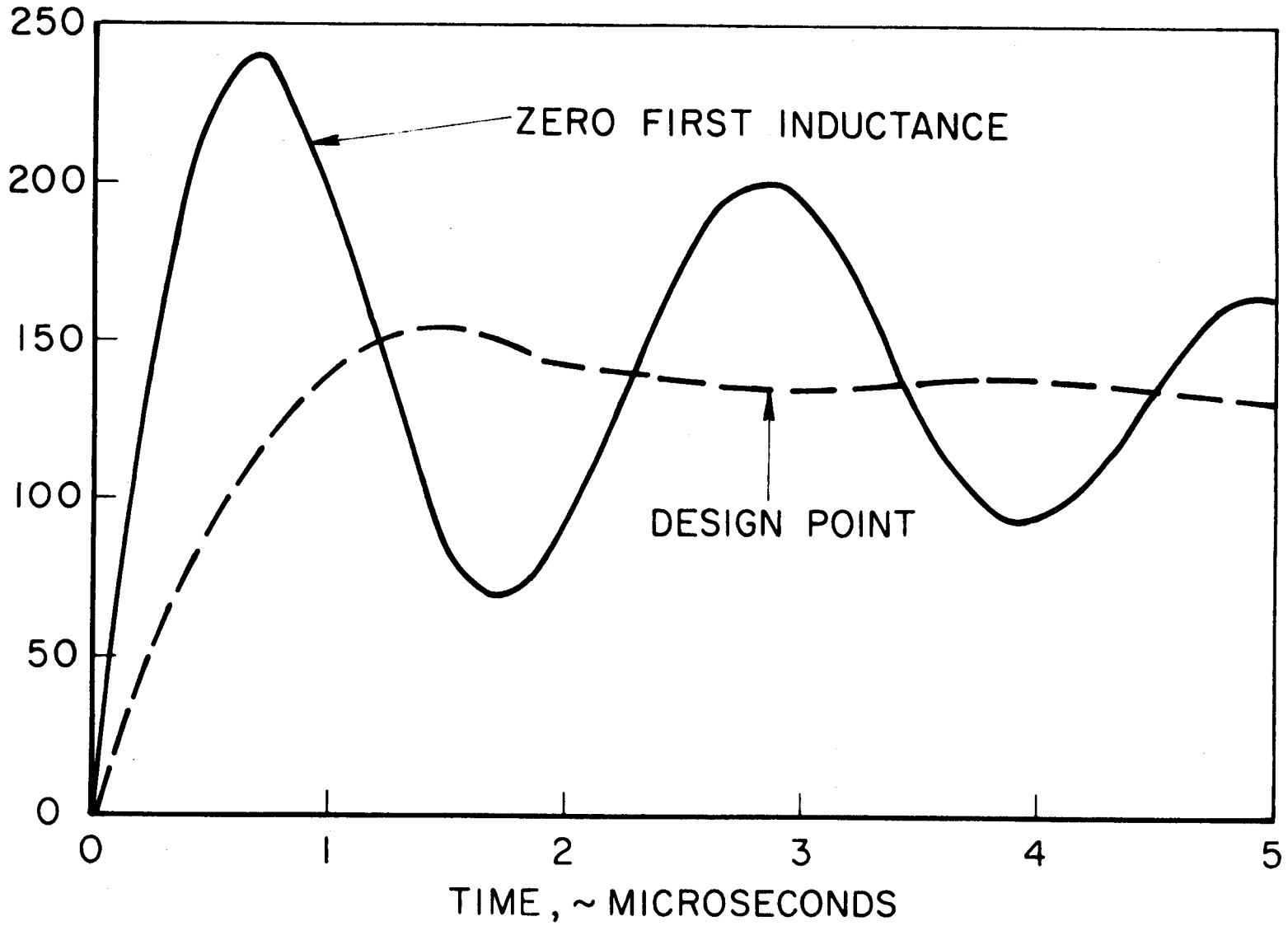

TYPICAL 5-SECTION CURRENT WAVE FORMS

FIGURE 25